Theses and Dissertations   Thesis Collection

1964

An investigation of the prerotation characteristics of a fluid in the intake duct of a centrifugal pump

Osgood, Wayne R.

Monterey, California: U.S. Naval Postgraduate School

http://hdl.handle.net/10945/28316

AN INVESTIGATION OF THE
PREROTATION CHARACTERISTICS OF A FLUID
IN THE INTAKE DUCT OF A CENTRIFUGAL PUMP

WAYNE R. OSGOOD

AN INVESTIGATION OF THE PREROTATION CHARACTERISTICS

OF A FLUID IN THE INTAKE DUCT OF A CENTRIFUGAL PUMP

* * * * *

Wayne R. Osgood

AN INVESTIGATION OF THE PREROTATION CHARACTERISTICS

OF A FLUID IN THE INTAKE DUCT OF A CENTRIFUGAL PUMP

by

Wayne R. Osgood

Lieutenant, United States Navy

Submitted in partial fulfillment of

the requirements for the degree of

MASTER OF SCIENCE
IN
AERONAUTICAL ENGINEERING

United States Naval Postgraduate School
Montery, California

1964

AN INVESTIGATION OF THE PREROTATION CHARACTERISTICS

OF A FLUID IN THE INTAKE DUCT OF A CENTRIFUGAL PUMP

by

Wayne R. Osgood

This work is accepted as fulfilling

the thesis requirements for the degree of

MASTER OF SCIENCE

IN

AERONAUTICAL ENGINEERING

from the

United States Naval Postgraduate School

ABSTRACT

The direction of flow along the centerline of several sections
of the inlet duct of a centrifugal pump was determined using a hot wire
anemometer. In contrast to other tests of this kind, the pump was
operated with air to facilitate the measurements. The present investi-
gation is part of a program at the U. S. Naval Postgraduate School to
evaluate the performance of liquid pumps with air in order to apply
aerodynamic measuring methods and equipment to the task. Data were
taken with the pump operating at different points on the characteristic
curve. The flow direction data are presented as a function of position
in the intake duct for various operating conditions.

Prerotation was observed, the character of which was in agreement
with theoretical predictions in that prerotation was in the same direc-
tion as the impeller rotation at the low flow rates and in the opposite
direction at the high flow rates. Backflow near the periphery of the
duct was observed at the low flow rates.

TABLE OF CONTENTS

LIST OF ILLUSTRATIONS

Symbol	Definition	Units
A	Cross sectional area of discharge pipe	ft^2
A_2	Outlet area of impeller	ft^2
b	Blade height at discharge of impeller	ft
D	Diameter of discharge pipe	ft
D	Diameter of hot wire	ft
D_2	Diameter of impeller at discharge	ft
g	Gravitational constant---32.174	ft/sec^2
I	Current through hot wire	amp
L	Length of hot wire	ft
n	Number of blades on impeller	
p	Static pressure of cooling gas	lb/ft^2
P_2	Outlet flange static pressure	lb/ft^2
P_s	Static pressure	in. H_2O
P_t	Total pressure	in. H_2O
P_s'	Static pressure in discharge pipe	lb/ft^2
q_o	Free stream dynamic pressure	in. H_2O
R	Gas constant for air ---53.35	$\dfrac{ft\ lb}{lbm\ ^oR}$
R	Resistance of hot wire	ohms
r	Distance from axis of pump of element considered	ft
r_i	Inner radius of channel	ft
r_o	Outer radius of channel	ft
R_o	Reference resistance of hot wire	ohms
Re	Reynolds Number in discharge pipe	
Rex	Modified Reynolds Number in discharge pipe	
T	Temperature of the hot wire	^oF

T_o	Reference temperature of hot wire	^oF
T_2	Total temperature at flow meter	^oR
U_2	Peripheral speed of impeller	ft/sec
V	Velocity in discharge pipe	ft/sec
V_e	Effective cooling velocity of cooling gas	ft/sec
V_{m2}	Meridianal velocity at discharge of impeller - $\mathbb{F}/A_2$	ft/sec
$\mathbb{F}$	Volume flow rate at discharge of impeller - $w/g\rho_2$	ft^3/sec
w	Mass flow rate	lbm/sec
α_1	Flow angle with respect to axial direction	radians
α_o	Reference temperature coefficient of resistivity	$^oF^{-1}$
β	Angle between hot wire axis and direction of cooling gas flow	degrees
β_{2B}	Exit blade angle	degrees
ΔP	Pressure rise - Ambient to outlet flange	lb/ft^2
$\Delta P'$	Apparent dynamic pressure in flow meter	lb/ft^2
$\mathfrak{f}$	Flow meter calibration factor	
θ	Angular displacement from directly into stream of static port on circular cylinder	radians
μ	Absolute viscosity in discharge pipe	lbm/ft sec
μ_B	Busemann slip factor	
μ_S	Stodola slip factor	
ρ	Density at flow meter	lbm/ft^3
ρ_2	Outlet density $\quad P_2/gRT_2$	$slugs/ft^3$
ϕ_2	Flow coefficient $\quad V_{m2}/U_2$	
ψ_2	Pressure coefficient $\quad \Delta P/\rho_2 U_2^2$	

AN INVESTIGATION OF THE PREROTATION CHARACTERISTICS

OF A FLUID IN THE INTAKE DUCT OF A CENTRIFUGAL PUMP

1. Introduction.

It has been observed for many years that rotation of fluid in the inlet ducts ahead of an impeller exists. This rotation may be in the same direction as, or opposite to, the direction of rotation of the impeller. The effect is more pronounced and easily observable at off design conditions but may even occur at the design point. It is essential to know the fluid angles at the impeller inlet in order to properly design the inlet blade angles. If the blade angle is very different from the relative flow angles, local high fluid velocities may produce the phenomenon of cavitation. While some cavitation may be tolerated to achieve higher flow rates, it is generally undesirable because it is destructive and causes inefficient and unstable operation of the pump.

The cause of the phenomenon o prerotation is somewhat obscure and little quantitative data is available to pump designers. Although conventional hydraulic pumps have been examined for prerotation, there do not exist prerotation data in the literature for the very small blade angles encountered in rocket fuel and oxidizer pumps. Experiments that have been done generally have used liquid pumps with water as the working fluid. It will be seen that the same results may be obtained using a liquid pump but with air as the working fluid. The latter would require much less power to drive it, less elaborate experimental equipment, and would provide easier ways to investigate the physical aspects of the process.

2. The Pump.

The pump used for this experiment was a liquid fuel pump for the Titan I missile. It is a centrifugal pump seven inches in diameter at

the eye and 11 inches at the discharge of the impeller. It has a diffuser with four vanes, an annular collector and a three inch diameter discharge flange. There is a static pressure tap at the discharge flange where the pressure, P_2, was taken. The impeller has two blades at the eye with additional blades starting at larger radii for a total of eight blades at the discharge. Figs. 1, 2, 3. The pump was driven by an air turbine.

3. The Inlet Duct.

The inlet duct consisted of a seven inch diameter, four inch long plexiglas spacer, a seven inch diameter, 24 inch long steel tube and a built up wooden bell mouth. Through the plexiglas, qualitative observations of the flow were made using smoke and cotton tufts. Mounted on the steel tube were four brackets with a hole through the pipe wall, through which a probe could be inserted to make a survey of the flow along the centerline of the pipe, top to bottom. These survey points were six inches apart, with the nearest one to the impeller being seven inches from the inlet flange. This point is referred to as position number four.

4. The Discharge Pipe.

The discharge pipe was a three inch pipe, ten feet long. It had a bundle of one-half inch copper tubing six inches long at the pump end to act as a flow straightener. Five feet from the pump was a flow meter consisting of a total pressure Kiel probe with a thermocouple mounted at the centerline of the pipe and two static ports on opposite sides of the pipe. For calibration of the flow meter see Appendix C. At the discharge end of the pipe was a gate valve for controlling the flow rate.

5. The Hot Wire Anemometer.

A Flow Corporation, Model HWB, hot wire anemometer was used to determine flow direction using a .00035 inch diameter tungsten wire. The probe was mounted in a protractor which in turn was mounted on a slide. The depth of the hot wire could be determined by a scale on the slide and the directional orientation of the hot wire could be read to 0.2 degrees using a vernier scale on the protractor. The centerline of the inlet duct at position number two at the highest flow rate was used as a calibration point for directionally orienting the hot wire.

6. Other Equipment.

An electronic counter was used to determine pump speed. A bank of vertical tube manometers was used to measure pressures in cm. of water. The differential pressure was measured with a water micromanometer. Discharge total temperature was determined with a Brown thermocouple instrument. A four-foot cubic plywood box was used as an inlet plenum to act as a buffer between the inlet duct and ambient turbulence. The inlet to the plenum was a two-foot square hole covered with four layers of filter cloth.

7. Speed of the Pump.

The design speed of the pump is 14,000 RPM. It was originally planned that several speeds in the neighborhood of the design speed would be used for this experiment. Upon running the pump at speeds of 10,000 to 12,000 RPM, large amplitude vibrations were observed. A dynamic balance of the air turbine failed to lessen the vibrations so a speed of 8,800 RPM was settled upon for the tests. The vibrations are evidently due to the ball bearings whose axial loading is not as great as design loading because air is the fluid being pumped.

In order to avoid cavitation the axial velocity ahead of the pump is kept small. The reduction in RPM produced a further decrease in velocity which caused difficulty in measuring the dynamic pressure in the duct.

8. Measuring the Flow Angle.

The first attempt at measuring the flow direction in the inlet duct was made utilizing a United Sensor airflow probe. This probe had five pressure ports. When the probe was properly oriented in the air stream, one would measure the total pressure, two would measure the static pressure, and two others not used in this application could be used to measure components of the flow in the direction of the probe axis. After calibration in an air stream of known direction, the probe could be used to determine the direction of airflow in the inlet duct. Not only the direction, but also the velocity of the flow could be determined at any point in the duct tested, and from this the flow rate could have been calculated.

The very low flow rates made the pressure measurements to determine flow angles very critical. The maximum flow rate which was measured later with a flow meter was .46 lb/sec. This flow rate, assuming a uniform velocity distribution in the inlet duct, would yield a dynamic head of about 0.1 inches of water. Consider now the ideal flow about a cylinder where

$$P_s - P_t = q_o(1-4\sin^2\theta) = 0.1(1-4\sin^2\theta)$$

then $\quad \dfrac{dP_s}{d\theta} = -0.8 \sin\theta\cos\theta$

for $\quad \theta = 45^o$

$\dfrac{dP_s}{d\theta} = -0.4 \text{ in.H}_2\text{O/radian} = -0.007 \text{ in.H}_2\text{O/degree}$

Hence, if the probe were one degree away from facing directly into the stream, the pressure difference between the two static ports would be about .015 inches of water. An inclined manometer was available which could be read to .01 inches. However, since the sensitivity goes down even further as the flow rate is reduced, it was felt that the accuracy of results would be rather poor with this method.

The hot wire anemometer offered a possible solution. As pointed out in Appendix D, the directional sensitivity of the hot wire is greatest when the wire axis is aligned with the direction of flow. It was felt that the supporting pin ahead of the wire might cause turbulence and shield the flow from the full effect of the cooling gas stream. To avoid this, the leading end support pin was filed off so that the wire, when soldered across the tips of the pins, made an angle of about 65° with the probe axis. No apparent reduction in the galvanometer needle fluctuations was noted. Since the directional sensitivity of the probe is reduced by this technique, the standard probe was used.

The hot wire anemometer, being sensitive enough to detect very small velocities, is also sensitive to perturbation velocities. Therefore, it became necessary to build the intake plenum chamber, described in Sec. 6, to prevent ambient turbulence from giving an indication of a change in flow direction. Even with the plenum chamber there was always some fluctuation of the galvanometer needle used to determine the resistances. With fluctuations of the needle it was difficult to find a maximum, so the scheme actually used was to record the two angles, 15-20 degrees on either side of the angle for maximum deflection, which produced the same galvanometer reading. The angle halfway between the two recorded was then used as the flow angle. In this technique there

can be no shielding by the upstream supporting pin because it is not directly in front of the wire.

9. Existing Theories.

While the exact mechanism of prerotation is not clear, the phenomenon has been observed by many investigators for years. [6]. Several attempts have been made to explain the reasons for prerotation. At off design conditions the fluid is said to acquire prerotation by taking the path of least resistance or least inlet impact. For flow rates lower than design the flow acquires prerotation which is the same direction as the impeller rotation, a positive prerotation, and at flow rates higher than design the prerotation is negative. [5]. Backflow in the outer portion of the impeller channel at low flow rates, and high net heads are believed to be the cause of positive prerotation. Backflow has been observed in the inlet duct and in the diffuser. [4].

The impeller discharge conditions seem to have a great deal of influence on prerotation. Experiments at California Institute of Technology using a vaneless, symmetrical diffuser showed practically no evidence of prerotation over the entire range of flow rates. [2]. This pump did show a positive component of tangential velocity at the discharge of the impeller when operating at zero pressure coefficient. This positive angular momentum at the discharge would seem to indicate a positive rotation at the inlet, but no such rotation was observable. At zero pressure coefficient the accepted theory would predict a negative prerotation. Shepherd believes that the positive angular momentum at the discharge is due to losses in the impeller. [5].

The pump studied by Peck had a vaneless diffuser, but had the typical eccentric discharge volute. [4]. This pump exhibited considerable

6

prerotation and backflow at low flow rates. It showed no negative
prerotation at flow rates above the design point.

Existing theories, therefore, seem to be of little practical use
to the pump designer. The discharge conditions evidently are a contrib-
uting influence on prerotation.

10. Results.

The results of these tests are tabulated in Tables 1 through 22
and are presented in graphical form in Figs. 8 through 17.

11. Discussion.

Fig. 8 is the experimentally determined characteristic curve of
the pump. The pressure coefficient used here is non-dimensional and
is defined as follows:

$$\psi_2 = \Delta P / \rho_2 U_2^2$$

where, ρ_2 is a derived density using the static pressure at the outlet
flange and the total temperature at the flow meter. The flow coefficient
is also non-dimensional and is defined as follows:

$$\phi_2 = V_{m2}/U_2$$

V_{m2}, not being measured directly, is a derived quantity using the
measured flow rate, w, the density, ρ_2, and outlet area of the impeller.
The outlet area does not consider any restriction by the blades and is
merely $\pi D_2 b$.

$$V_{m2} = w/\rho_2 \pi D_2 b$$

The theoretical pressure coefficients as a function of the flow
coefficient were computed using the slip factors of Stodola and Busemann.
These are plotted in Fig. 6 for reference. The Stodola slip factor, μ_s,
was calculated using his equation: [5]

$$\mu_s = 1 - \frac{\pi \cos\beta_{2B}}{n} = \frac{V_{u2}}{V_{u2} \text{ (theoretical)}}$$

Busemann's slip factor, μ_B, for eight blades and an exit blade angle
of $-73.75°$, Fig. 3, was obtained from a graph in Ref. 5. The theoretical
pressure coefficient then may be expressed as:

$$\Psi_{2S,B} = \mu_{S,B} + \phi_2 \tan\beta_{2B}$$

The efficiency may be expressed as the ratio of actual to theoret-
ical pressure coefficients. The efficiency was calculated and plotted
in Fig. 7. The pressure coefficients and efficiency can be expected to
increase somewhat with the liquid fuel as a working fluid due to increased
Reynolds number.

The prerotation observed in these tests is generally what would be
predicted by accepted theories. Positive prerotation and backflow in
the outer portions of the inlet duct were observed at low flow rates.
Positive prerotation is indicated in the figures as an angle greater
than zero for depths less than three and one half inches and an angle
less than 360 degrees for greater depths.

There is considerable scatter in the data with respect to the flow
angle. Several repeatability tests were made during the course of the
experiment which indicated that the data should be accurate to within
one degree. These tests were performed in connection with the direc-
tional calibration of the hot wire. Each time the wire had to be
replaced it was necessary to establish a new angular tare. Since this
was a one time measurement which effected all the readings taken with
that wire, it was considered worthwhile to use an average of eight to
ten readings rather than just one. No readings were more than one degree
different from the average. However, these tests were made on the
centerline of the inlet duct at position number two with the pump
operating at maximum flow coefficient. Directional sensitivity of the
hot wire is proportional to the velocity so that the accuracy would be

poorer at the lower flow rates. Velocity perturbations in any direction would give an indication of a change in flow direction to the observer. It can reasonably be expected that these perturbations would be oscillatory in character, however.

Increasing the speed of the pump to 14,000 RPM would considerably increase the accuracy of the data. Directional sensitivity is proportional to the velocity with the hot wire anemometer and proportional to the square of the velocity if the pitot-static tube is used. Velocity is proportional to the RPM. Perturbation velocities would probably not increase as much so the fluctuations of the needle would be reduced also.

In spite of the scatter, it is felt that some negative prerotation was present at the high flow rates. In Fig. 17, an interpretation has been made which shows a maximum of two degrees of negative prerotation at the maximum flow rate.

At the apparent design point there is still considerable positive prerotation and backflow. The point of highest efficiency is at a flow coefficient of .03. Fig. 12, showing data taken at a flow coefficient of .048, shows that positive prerotation and backflow were observed at position number four.

Velocity measurements were not taken so the exact incidence angles cannot be calculated. However, by assuming that the magnitude of the velocity is a constant across the section for each flow rate, an estimate of the effect of prerotation on the incidence angles may be made. This was done for the two extreme flow rates. The following analysis was made to determine the velocities in the inlet duct for the case with prerotation and for the case of axial flow with uniform velocity distribution for comparison.

9

$$V^{\cdot} = \phi_2 U_2 A_2 = 2\pi V \int_{r_i}^{r_o} r \cos\alpha_1 \, dr$$
$$= 2\pi V \sum_{j=1}^{n} r_j \cos\alpha_{1j} \, \Delta r_j$$

for the axial flow case

$$\phi_2 U_2 A_2 = \pi V (r_o{}^2 - r_i{}^2)$$

The results were:

$\phi_2 = .026$ $V_{(with\ rotation)} = 33.6$ ft/sec

                     $V_{(axial\ flow)} = 7.1$ ft/sec

$\phi_2 = .097$ $V_{(with\ rotation)} = 31.2$ ft/sec

                     $V_{(axial\ flow)} = 26.4$ ft/sec

These results were used in plotting the velocity triangles in Figs. 19 through 22.

It can be seen that, except for the very large amounts of prerotation at the low flow rate, velocity of the flow has a greater influence on the incidence angles than the flow angle itself. Of course, these velocities must be greater with prerotation than without for any given flow rate. Therefore, the tendency to cavitate would be greater with prerotation because the increased velocities produce reduced static pressures.

12. Conclusions.

These tests show essentially the same trends as other tests have shown where water was used as the working fluid.

The very small velocities involved may be handled very well with the hot wire anemometer. This instrument may be used to measure the velocity as well as the flow direction. Appendix D.

Testing liquid pumps with air has many advantages. The power requirements for driving the pump are less. Return and supply lines with their accompanying pumps and coolers are not required. Measuring

equipment is not subjected to high dynamic loads. Test setups may be kept simple and aerodynamic measuring devices can be used. Packing is not required around the probe to prevent leakage and the unused holes in the inlet duct may be sealed with a piece of drafting tape.

13. Recommendations.

It is recommended that:

    a. Efforts be made to eliminate vibrations so that tests may be made at higher speeds. Preloading the bearings and a dynamic balance of the entire assembly should reduce vibrations. Installation in one of the new test cells in a more permanent fashion would eliminate feedback of vibrations from the supply line and the discharge pipe. Directional sensitivity of the hot wire is proportional to the velocity so this would improve the accuracy of the data.

    b. Velocity measurements as well as direction measurements be taken using the hot wire anemometer. Direction should be determined first and then velocity should be measured with the wire axis perpendicular to the air stream.

    c. A more sophisticated probe which employs two hot wires on the same probe be purchased or fabricated to try to obtain more accurate data.

    d. The diffuser vanes be removed to determine the effect of that section of the pump on the prerotation.

14. Acknowledgments.

The author acknowledges many helpful suggestions and assistance from fellow students and the laboratory staff. He wishes to thank the

BIBLIOGRAPHY

1. Ladenburg, R. W., B. Lewis, R. N. Pease and H. S. Taylor. Physical Measurements in Gas Dynamics and Combustion. Princeton University Press, 1954.

2. Osborne, W. C. and D. A. Morelli. Head and Flow Observations on A High Efficiency Free Centrifugal Pump Impeller. Transactions, American Society of Mechanical Engineers, v. 72, 1950: 999-1007.

3. National Advisory Committee for Aeronautics. An Investigation of Backflow Phenomenon in Centrifugal Compressors, by W. A. Benser and J. J. Moses. 1945. NACA report no. 806.

4. Peck, J. F. Investigations Concerning Flow Conditions in a Centrifugal Pump, and the Effect of Blade Loading on Head Slip. Institution of Mechanical Engineers, v. 164, 1951: 1-34.

5. Shepherd, D. G. Principles of Turbomachinery. The Macmillan Company, 1956.

6. Stepanoff, A. J. Turboblowers: Theory, Design, and Application of Centrifugal and Axial Flow Compressors and Fans. John Wiley and Sons, Inc., 1955.

7. Watson, R. M. Cavitation in Centrifugal Pumps - Some of the Less Well-Known Factors. Proceedings of the National Conference on Industrial Hydraulics. v. 1, October, 1947: 50-65.

APPENDIX A

TABLES

TABLE 1

PREROTATION TEST

RUN NO. 1   12 MARCH 1964

POSITION NO. 1

FLOW COEFFICIENT = .07594   PRESSURE COEFFICIENT = .27850

DEPTH	ANGLE
.10	355.40
.50	2.60
1.00	1.60
1.50	357.10
2.00	357.80
2.50	358.70
3.00	359.20
3.50	.20
4.00	359.60
4.50	1.40
5.00	1.80
5.50	.30
6.00	3.80
6.50	1.30
6.90	356.50

15

TABLE 2

PREROTATION TEST

RUN NO. 2   13 MARCH 1964

POSITION NO. 1

FLOW COEFFICIENT = .09598   PRESSURE COEFFICIENT = .08463

DEPTH	ANGLE
.10	.90
.50	1.20
1.00	2.00
1.50	355.60
2.00	357.00
2.50	359.60
3.00	2.70
3.50	.00
4.00	3.70
4.50	359.40
5.00	3.80
5.50	1.10
6.00	5.50
6.50	355.40
6.90	355.70

TABLE 3

PREROTATION TEST

RUN NO. 3   13 MARCH 1964

POSITION NO. 4

FLOW COEFFICIENT = .09590   PRESSURE COEFFICIENT = .08522

DEPTH	ANGLE
.10	1.90
.50	359.00
1.00	359.10
1.50	358.95
2.00	358.50
2.50	357.30
3.00	359.10
3.50	.95
4.00	.50
4.50	2.15
5.00	1.50
5.50	1.10
6.00	.20
6.50	358.70
6.90	359.20

TABLE 4

PREROTATION TEST

RUN NO. 4   13 MARCH 1964

POSITION NO. 4

FLOW COEFFICIENT = .06336   PRESSURE COEFFICIENT = .37310

DEPTH	ANGLE
.10	1.60
.50	359.70
1.00	.45
1.50	352.80
2.00	357.00
2.50	357.20
3.00	358.95
3.50	1.50
4.00	.35
4.50	359.40
5.00	358.75
5.50	.30
6.00	.15
6.50	359.90
6.90	356.55

18

TABLE 5

PREROTATION TEST

RUN NO. 5   13 MARCH 1964

POSITION NO. 4

FLOW COEFFICIENT = .02145   PRESSURE COEFFICIENT = .56532

DEPTH	ANGLE
.10	102.50
.50	97.00
1.00	84.60
1.50	67.20
2.00	45.90
2.50	27.95
3.00	12.20
3.50	1.30
4.00	353.30
4.50	340.45
5.00	322.40
5.50	299.40
6.00	280.20
6.50	264.95
6.90	256.10

TABLE   6

PREROTATION TEST

RUN NO.   6

POSITION NO. 4

FLOW COEFFICIENT = .04808   PRESSURE COEFFICIENT = .49974

CEPTH	ANGLE
.10	101.45
.50	95.00
1.00	78.25
1.50	55.70
2.00	21.50
2.50	9.50
3.00	2.80
3.50	360.00
4.00	358.00
4.50	354.10
5.00	341.40
5.50	321.00
6.00	289.70
6.50	267.75
6.90	252.30

TABLE 7

PREROTATION TEST

RUN NO. 7   17 MARCH 1964

POSITION NO. 4

FLOW COEFFICIENT = .06138   PRESSURE COEFFICIENT = .40929

DEPTH	ANGLE
.10	357.50
.50	357.60
1.00	354.90
1.50	355.60
2.00	357.30
2.50	357.30
3.00	356.50
3.50	.05
4.00	359.65
4.50	354.00
5.00	359.35
5.50	358.40
6.00	359.70
6.50	355.40
6.90	351.90

TABLE 8

PREROTATION TEST

RUN NO. 8   18 MARCH 1964

POSITION NO. 4

FLOW COEFFICIENT = .07989   PRESSURE COEFFICIENT = .27829

DEPTH	ANGLE
.10	.15
.50	.40
1.00	359.50
1.50	.10
2.00	358.85
2.50	359.90
3.00	.45
3.50	.40
4.00	.65
4.50	358.85
5.00	359.50
5.50	359.95
6.00	1.15
6.50	2.05
6.90	1.55

22

TABLE 9

PREROTATION TEST

RUN NO. 9   18 MARCH 1964

POSITION NO. 4

FLOW COEFFICIENT = .06496   PRESSURE COEFFICIENT = .40275

DEPTH	ANGLE
.10	3.45
.50	2.40
1.00	.90
1.50	358.80
2.00	359.60
2.50	359.35
3.00	358.90
3.50	359.70
4.00	1.00
4.50	.50
5.00	358.60
5.50	1.45
6.00	.75
6.50	2.80
6.90	.90

TABLE 10

PREROTATION TEST

RUN NO. 10   18 MARCH 1964

POSITION NO. 3

FLOW COEFFICIENT = .06543   PRESSURE COEFFICIENT = .40059

DEPTH	ANGLE
.10	2.60
.50	3.20
1.00	.70
1.50	358.55
2.00	359.40
2.50	357.05
3.00	359.15
3.50	359.55
4.00	359.10
4.50	1.95
5.00	.80
5.50	.50
6.00	359.60
6.50	1.85
6.90	.50

TABLE 11

PREROTATION TEST

RUN NO. 11   18 MARCH 1964

POSITION NO. 3

FLOW COEFFICIENT = .09707   PRESSURE COEFFICIENT = .08362

DEPTH	ANGLE
.10	1.10
.50	2.60
1.00	.50
1.50	358.25
2.00	359.10
2.50	359.00
3.00	359.60
3.50	.20
4.00	1.60
4.50	1.30
5.00	1.35
5.50	359.30
6.00	.45
6.50	359.30
6.90	.75

TABLE 12

PREROTATION TEST

RUN NO. 12   19 MARCH 1964

POSITION NO. 1

FLOW COEFFICIENT = .08693   PRESSURE COEFFICIENT = .20918

DEPTH	ANGLE
.10	4.10
.50	1.00
1.00	.50
1.50	357.40
2.00	2.10
2.50	357.00
3.00	358.20
3.50	359.50
4.00	359.50
4.50	.20
5.00	.10
5.50	359.50
6.00	358.10
6.50	359.05
6.90	358.50

TABLE 13

PREROTATION TEST

RUN NO. 13   24 MARCH 1964

POSITION NO. 1

FLOW COEFFICIENT = .03853   PRESSURE COEFFICIENT = .56494

DEPTH	ANGLE
.10	5.70
.50	5.50
1.00	3.00
1.50	2.20
2.00	1.20
2.50	355.80
3.00	352.50
3.50	353.30
4.00	357.80
4.50	357.90
5.00	359.80
5.50	.50
6.00	.70
6.50	359.60
6.90	355.30

TABLE 14

PREROTATION TEST

RUN NO. 14   31 MARCH 1964

POSITION NO. 2

FLOW COEFFICIENT = .09675   PRESSURE COEFFICIENT = .08516

DEPTH	ANGLE
.10	2.40
.50	4.50
1.00	2.20
1.50	358.00
2.00	356.30
2.50	358.60
3.00	359.70
3.50	.00
4.00	1.35
4.50	.20
5.00	3.00
5.50	1.80
6.00	359.40
6.50	358.70
6.90	357.00

TABLE 15

PREROTATION TEST

RUN NO. 15   31 MARCH 1964

POSITION NO. 2

FLOW COEFFICIENT = .07927   PRESSURE COEFFICIENT = .28404

DEPTH	ANGLE
.10	358.70
.50	358.90
1.00	357.70
1.50	.15
2.00	358.45
2.50	358.60
3.00	.10
3.50	358.60
4.00	.80
4.50	1.50
5.00	1.50
5.50	1.30
6.00	359.20
6.50	358.70
6.90	.45

TABLE 16

PREROTATION TEST

RUN NO. 16   1 APRIL 1964

POSITION NO. 2

FLOW COEFFICIENT = .06485   PRESSURE COEFFICIENT = .40481

DEPTH	ANGLE
.10	3.00
.50	1.90
1.00	359.35
1.50	358.30
2.00	358.40
2.50	358.90
3.00	.70
3.50	1.05
4.00	.40
4.50	.75
5.00	360.00
5.50	1.50
6.00	359.50
6.50	.90
6.90	1.30

TABLE 17

PREROTATION TEST

RUN NO. 17   1 APRIL 1964

POSITION NO. 2

FLOW COEFFICIENT = .04756   PRESSURE COEFFICIENT = .52388

DEPTH	ANGLE
.10	4.90
.50	359.60
1.00	.60
1.50	358.10
2.00	357.70
2.50	357.90
3.00	360.00
3.50	359.80
4.00	.30
4.50	.40
5.00	1.35
5.50	.30
6.00	.70
6.50	359.40
6.90	3.30

TABLE 18

PREROTATION TEST

RUN NO. 18   1 APRIL 1964

POSITION NO. 2

FLOW COEFFICIENT = .02765   PRESSURE COEFFICIENT = .60983

DEPTH	ANGLE
.10	104.30
.50	100.30
1.00	87.10
1.50	68.20
2.00	43.10
2.50	22.60
3.00	11.50
3.50	2.20
4.00	357.40
4.50	346.50
5.00	330.50
5.50	306.30
6.00	282.60
6.50	264.10
6.90	256.60

TABLE 19

PREROTATION TEST

RUN NO. 19   1 APRIL 1964

POSITION NO. 3

FLOW COEFFICIENT = .02663   PRESSURE COEFFICIENT = .60978

DEPTH	ANGLE
.10	103.80
.50	96.80
1.00	87.30
1.50	74.20
2.00	56.20
2.50	35.90
3.00	18.10
3.50	8.70
4.00	352.60
4.50	334.90
5.00	313.60
5.50	295.85
6.00	277.60
6.50	263.40
6.90	256.60

TABLE 20

PREROTATION TEST

RUN NO. 20   1 APRIL 1964

POSITION NO. 3

FLOW COEFFICIENT = .07792   PRESSURE COEFFICIENT = .29394

DEPTH	ANGLE
.10	2.40
.50	2.10
1.00	359.50
1.50	359.00
2.00	358.35
2.50	.20
3.00	.60
3.50	.30
4.00	1.30
4.50	.60
5.00	359.70
5.50	.80
6.00	359.80
6.50	360.00
6.90	359.60

34

TABLE 21

PREROTATION TEST

RUN NO. 21   2 APRIL 1964

POSITION NO. 3

FLOW COEFFICIENT = .08694   PRESSURE COEFFICIENT = .19722

DEPTH	ANGLE
.10	.10
.50	359.80
1.00	357.50
1.50	358.20
2.00	359.00
2.50	.60
3.00	360.00
3.50	.70
4.00	1.00
4.50	1.60
5.00	1.10
5.50	360.00
6.00	359.50
6.50	359.70
6.90	.20

TABLE 22

PREROTATION TEST

RUN NO. 22   2 APRIL 1964

POSITION NO. 4

FLOW COEFFICIENT = .08687   PRESSURE COEFFICIENT = .19671

DEPTH	ANGLE
.10	.90
.50	356.00
1.00	.50
1.50	358.60
2.00	359.00
2.50	359.10
3.00	359.50
3.50	1.10
4.00	.70
4.50	.10
5.00	359.60
5.50	359.10
6.00	.60
6.50	357.90
6.90	2.10

APPENDIX B

FIGURES
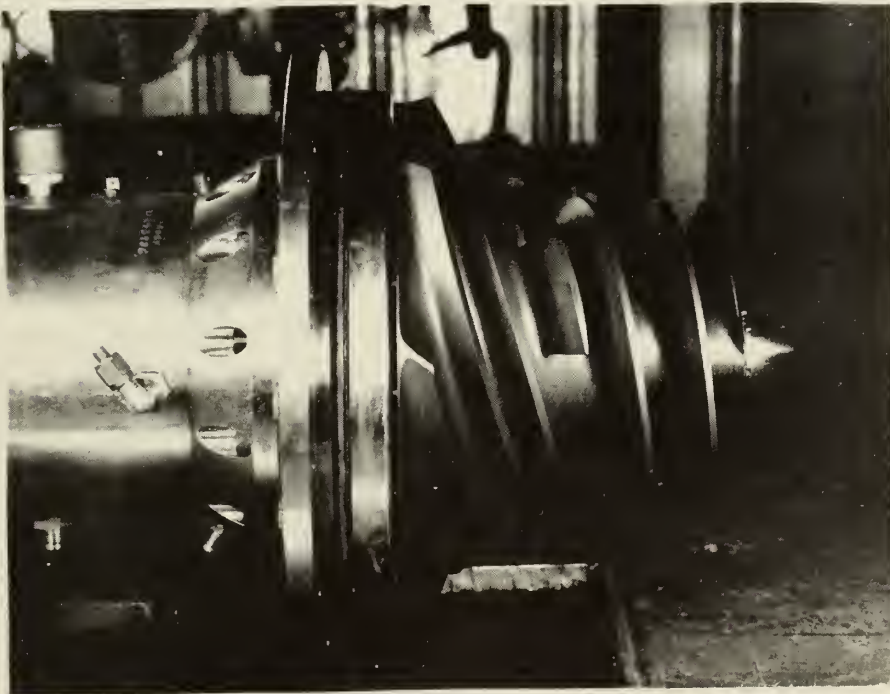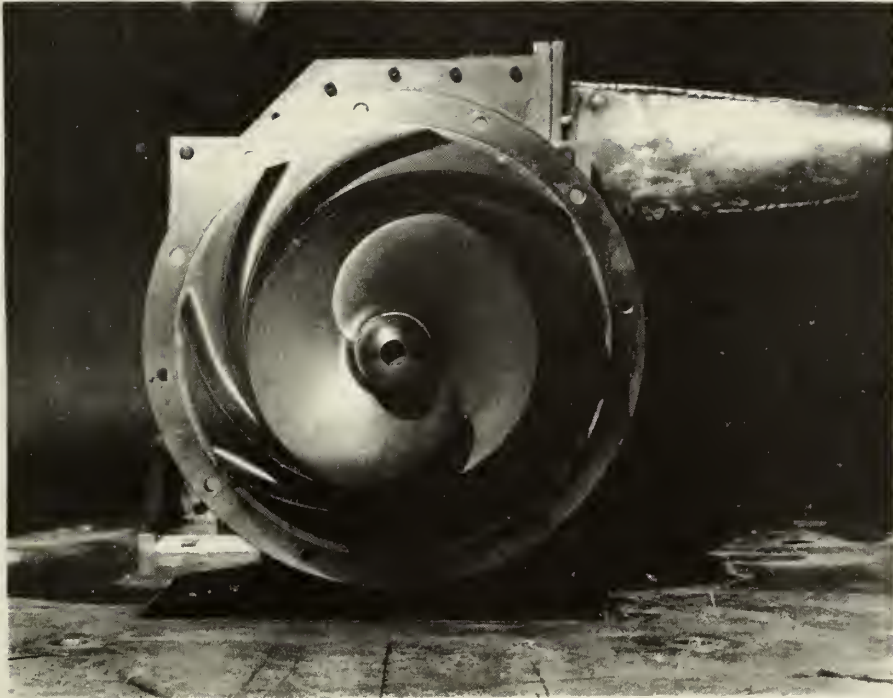
FIG. 1. Photographs of Impeller

38
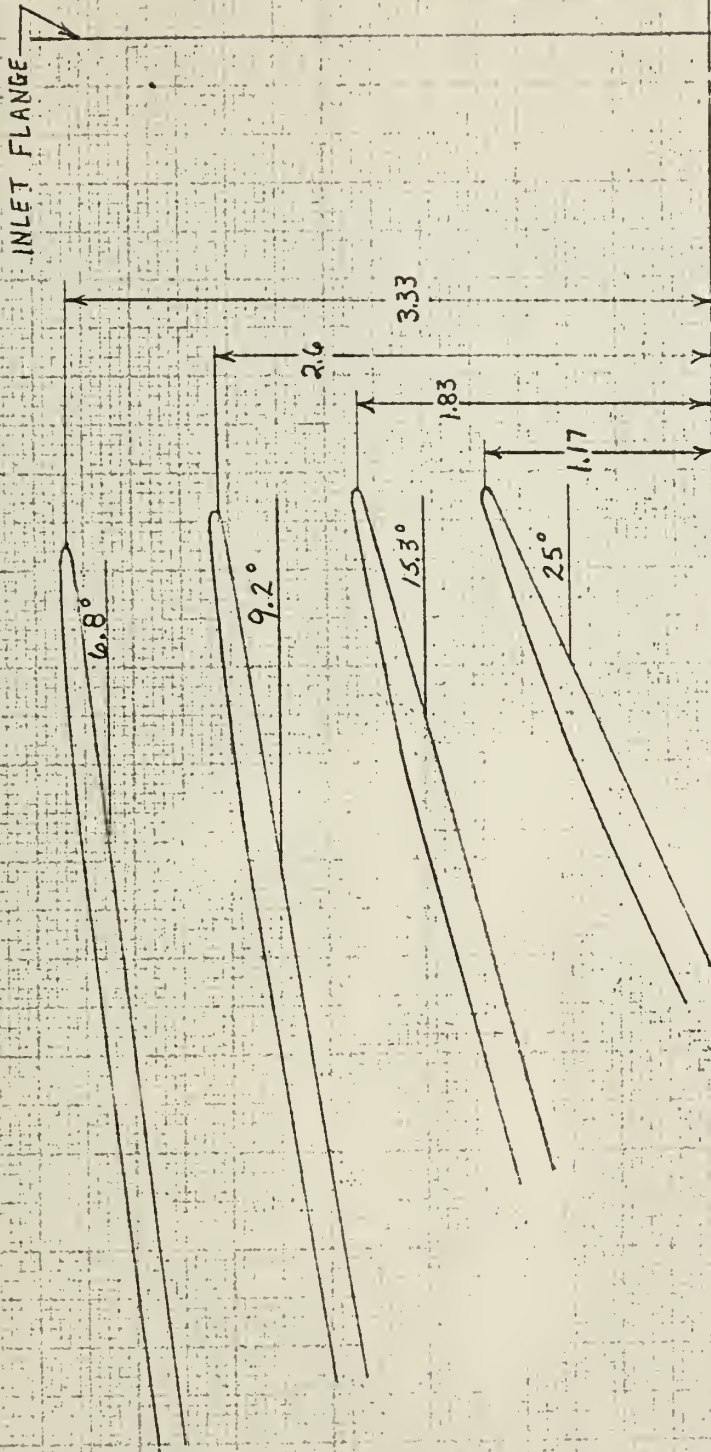
FIG. 2

INLET BLADE ANGLES

AT VARIOUS RADII

75.75°

VIEW FROM .A

A →

31°
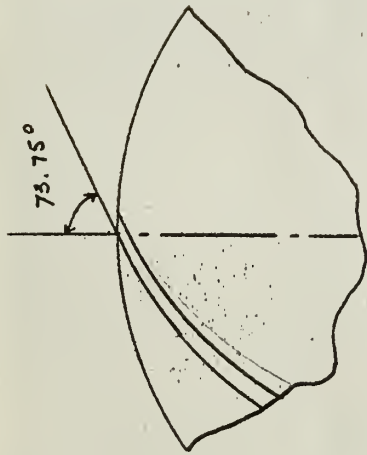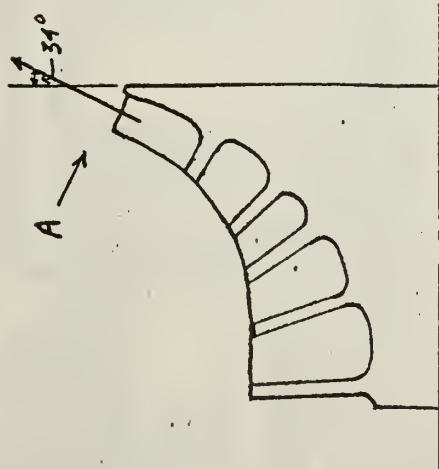
FIG. 3

EXIT BLADE ANGLES
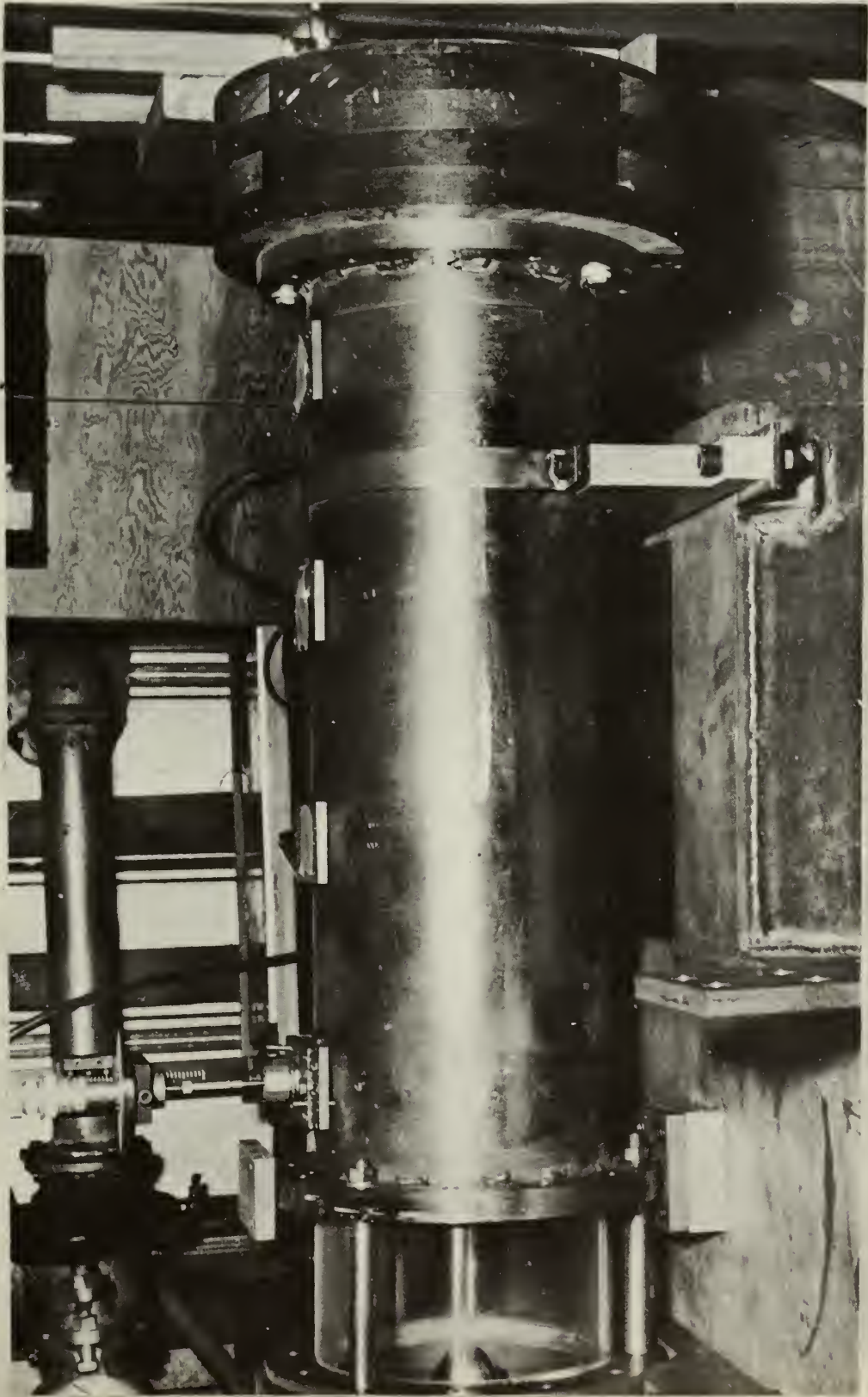
FIG. 4. Photograph of the Inlet Duct

41

FIG. 5. Photograph of the Flow Meter
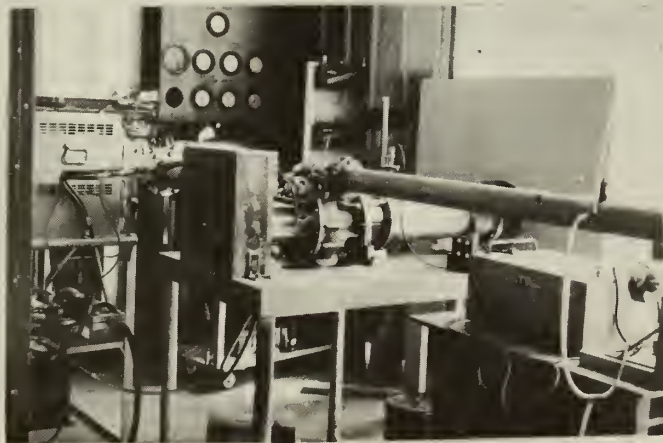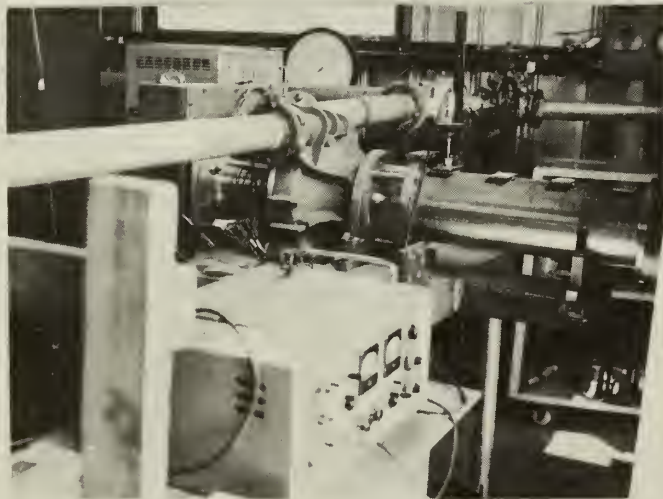
Fig. 6. Photographs of
Entire Test Setup

43

FIG. 7

INLET DUCT

FIG. 8
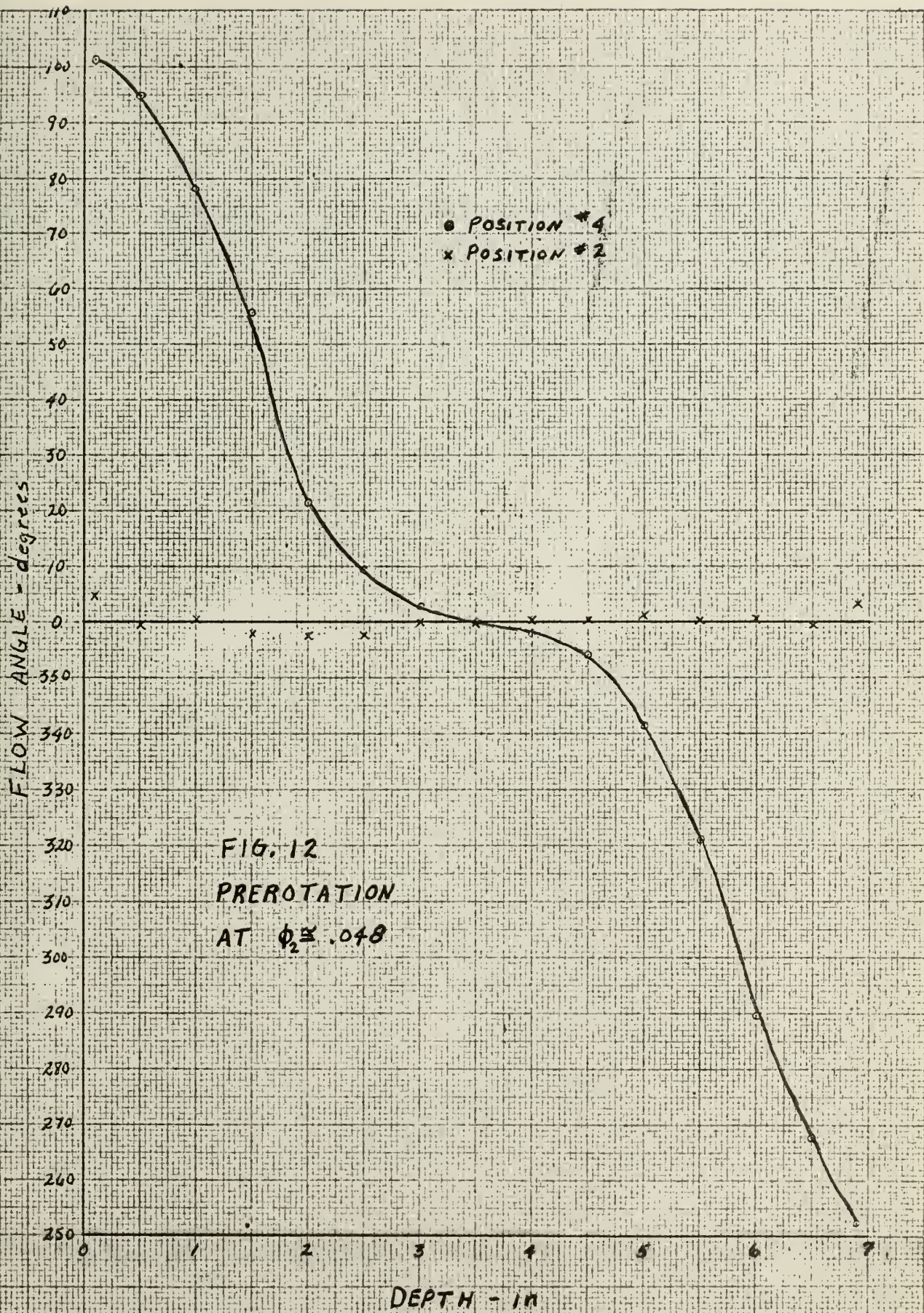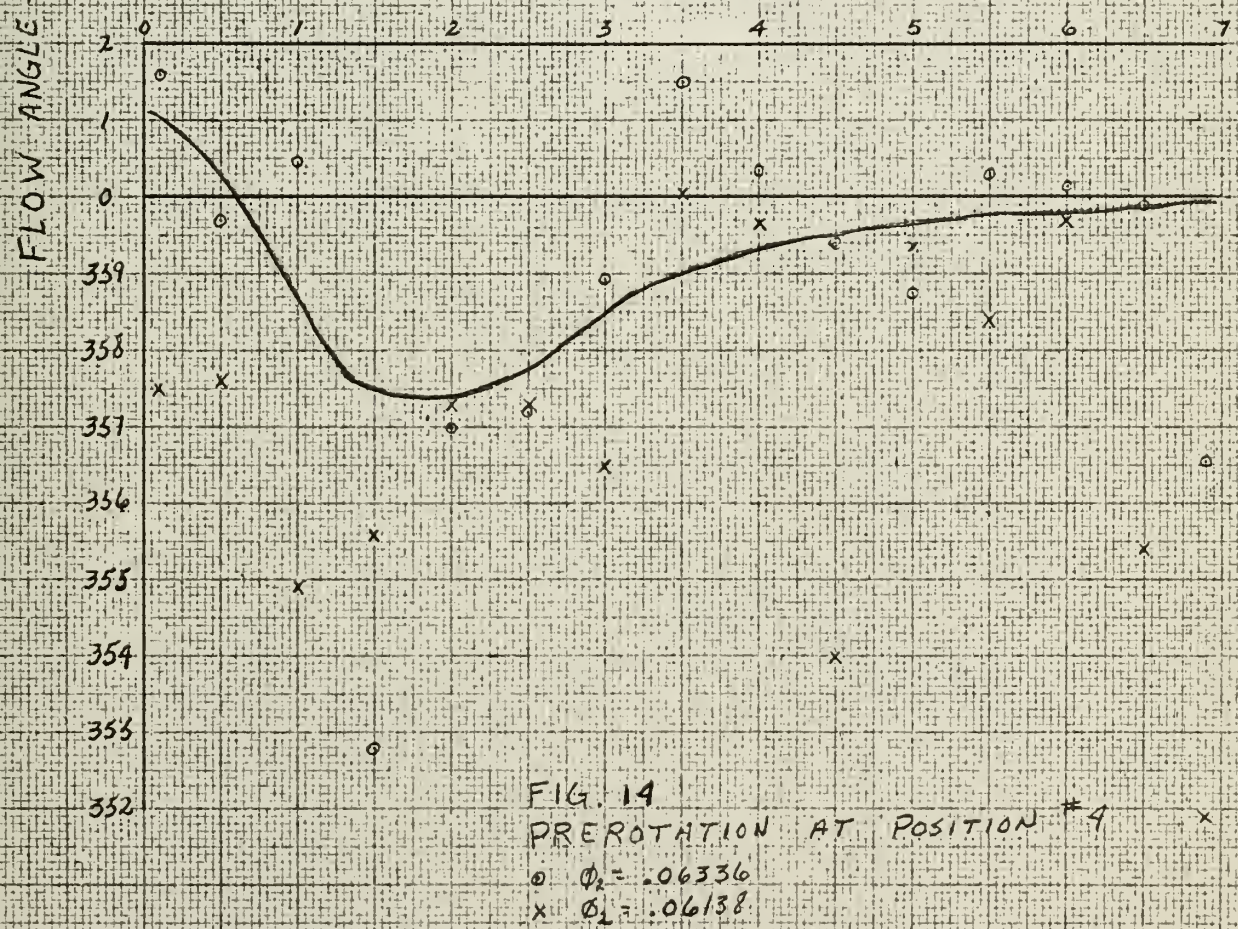PUMP CHARACTERISTIC CURVE
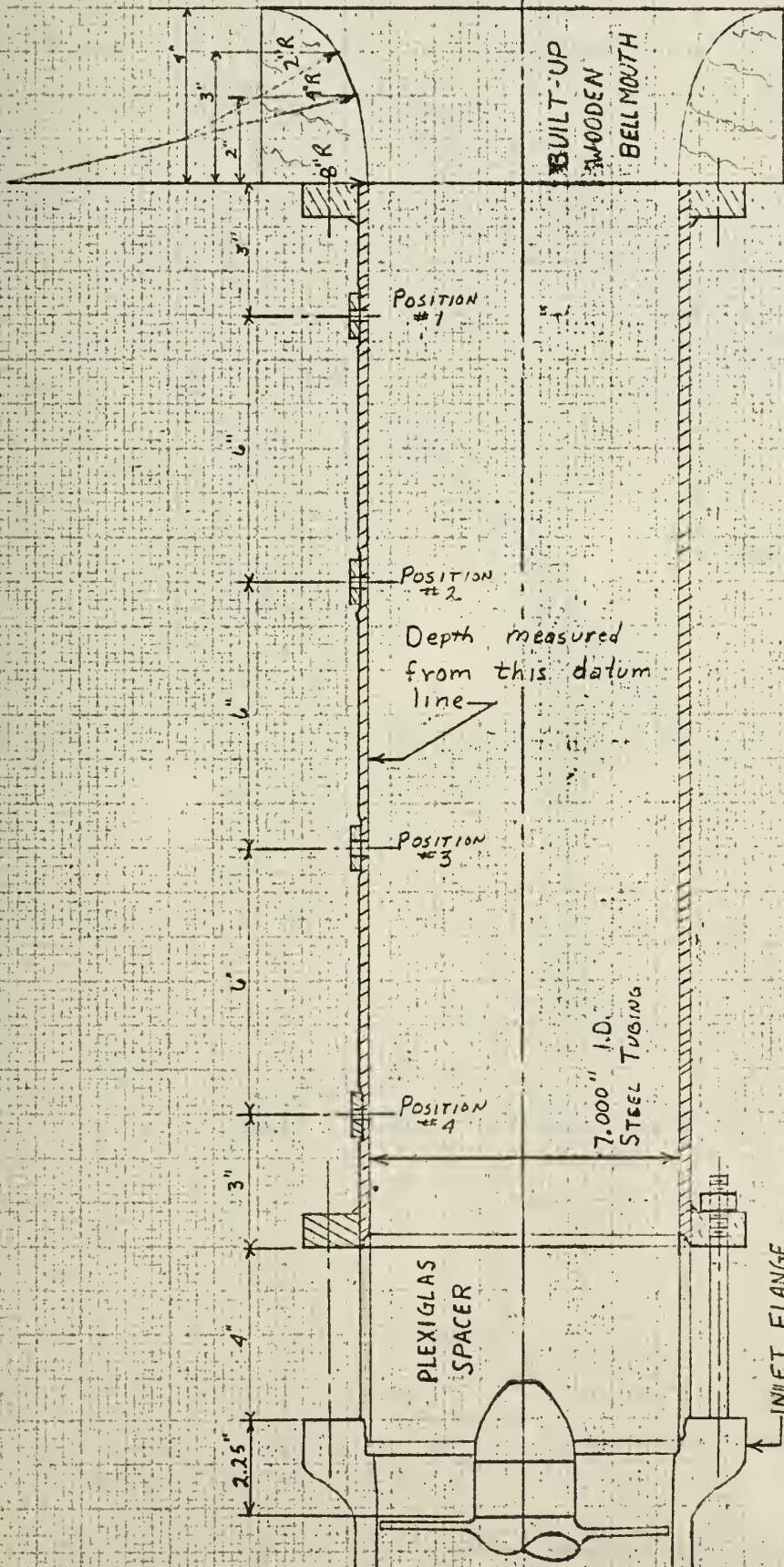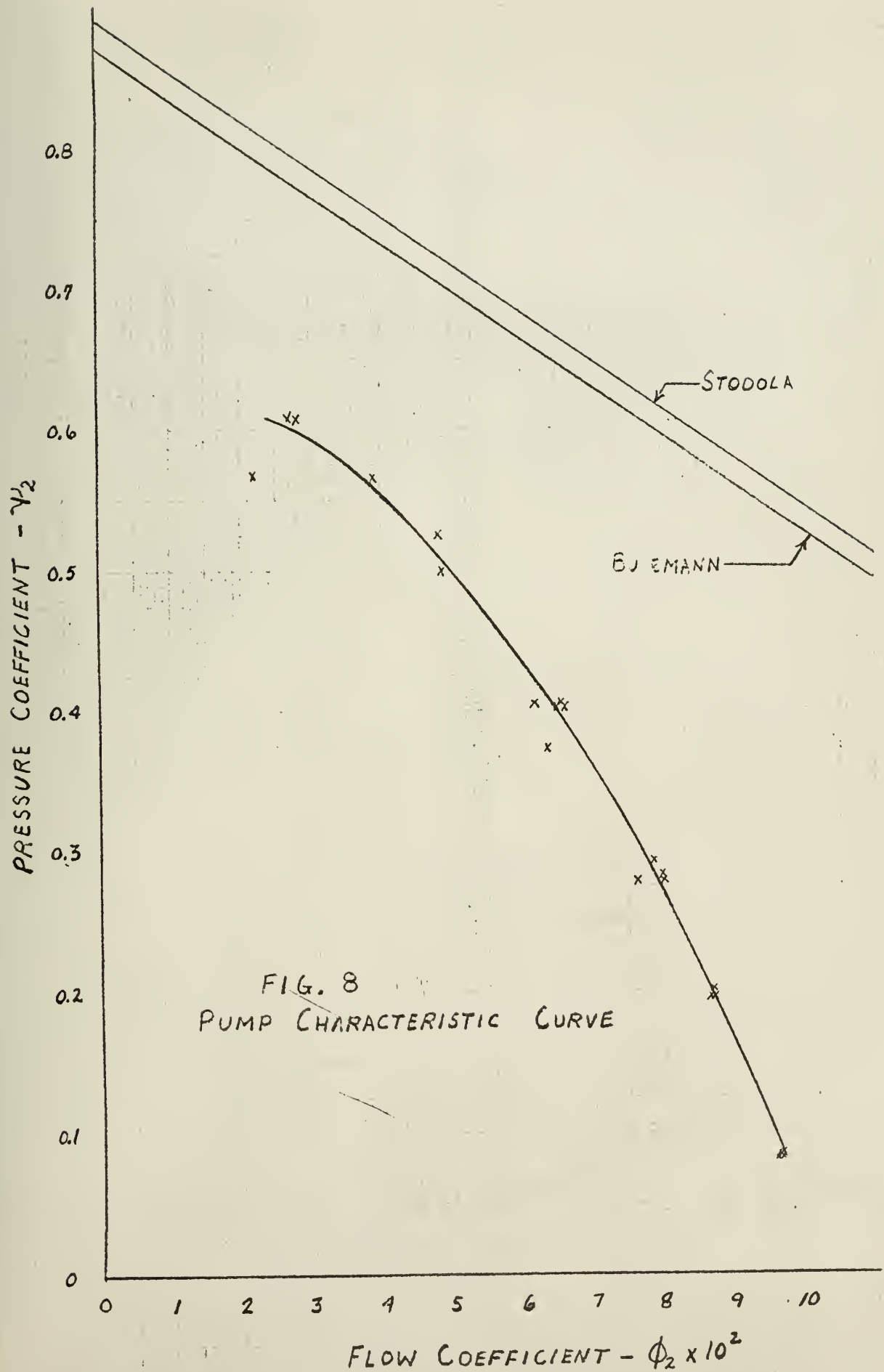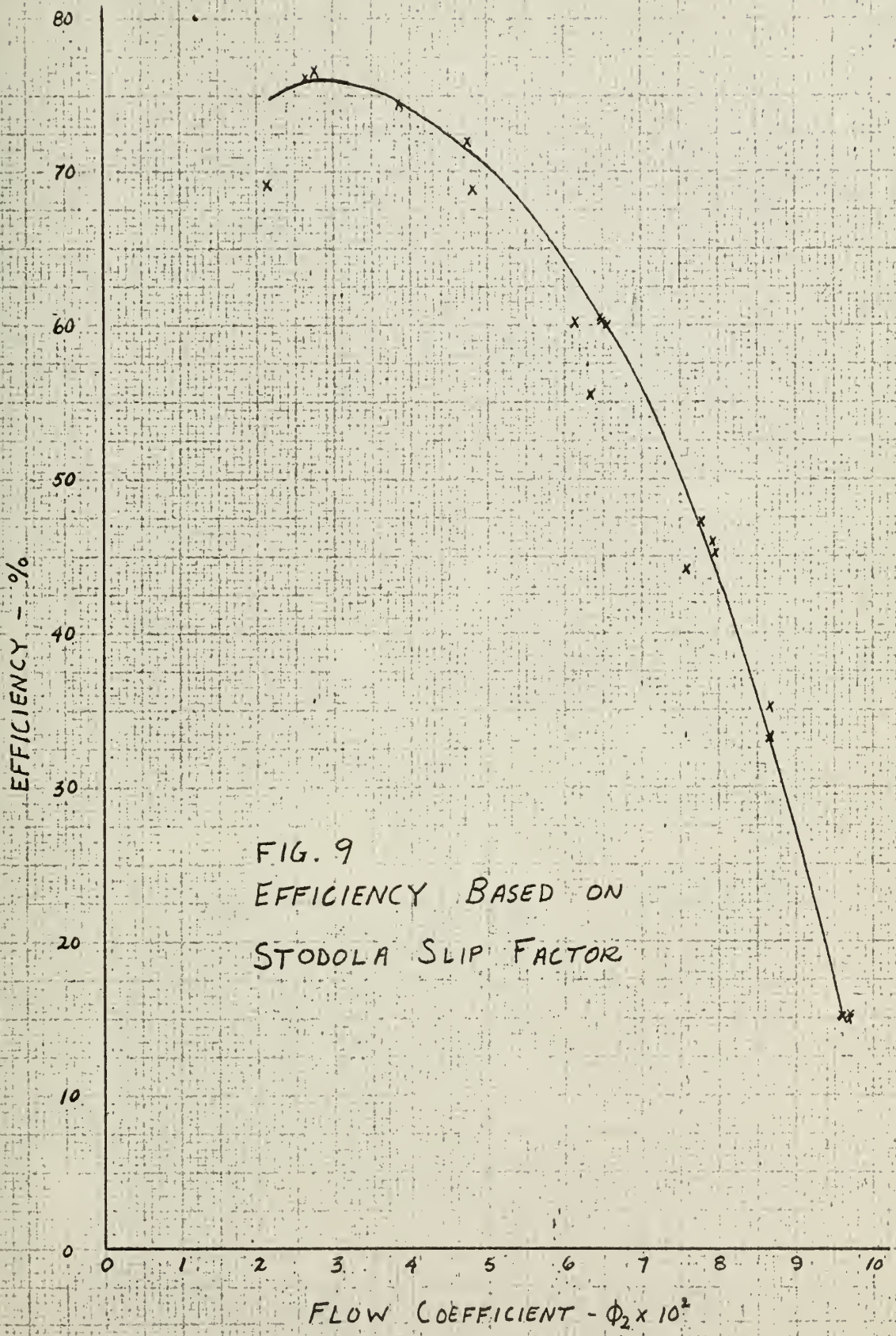
FIG. 9
EFFICIENCY BASED ON
STODOLA SLIP FACTOR

FIG. 10
PREROTATION AT LOW
VALUES OF FLOW COEFFICIENT

⊙ POSITION #4 $\phi_2 = .02145$
□ POSITION #3 $\phi_2 = .02663$
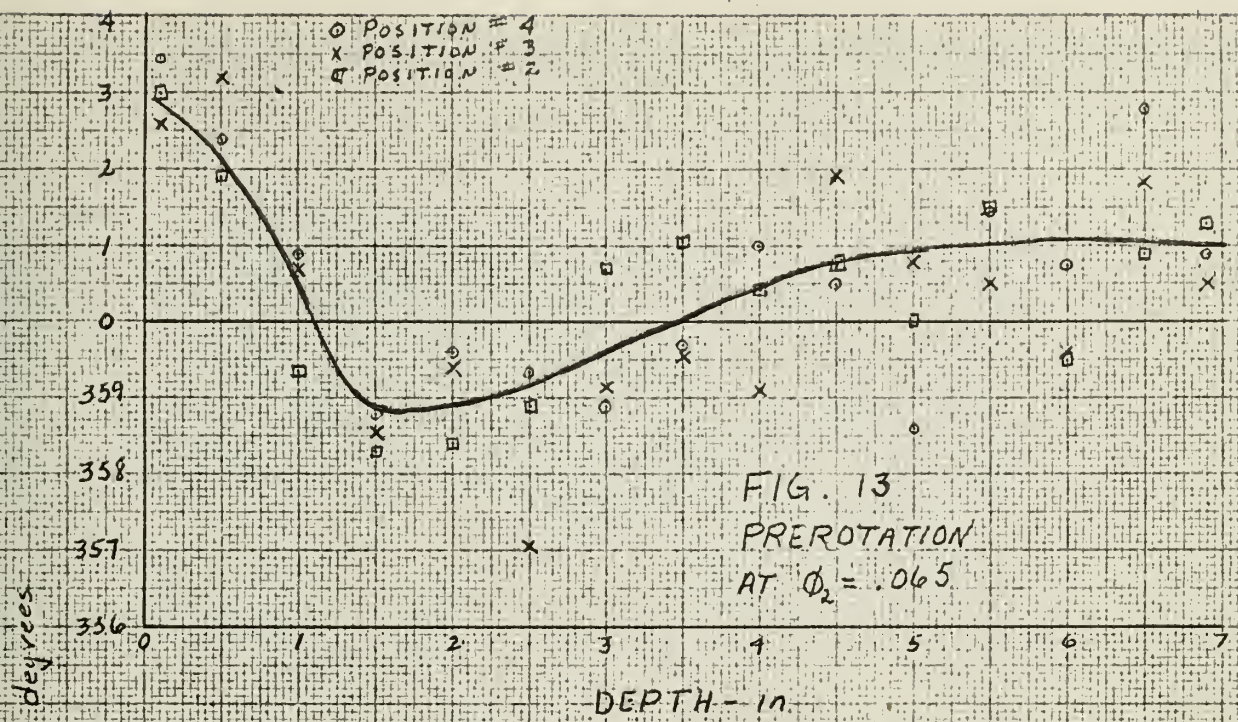× POSITION #2 $\phi_2 = .02765$

BACKFLOW
BACKFLOW

FLOW ANGLE – degrees

DEPTH – in
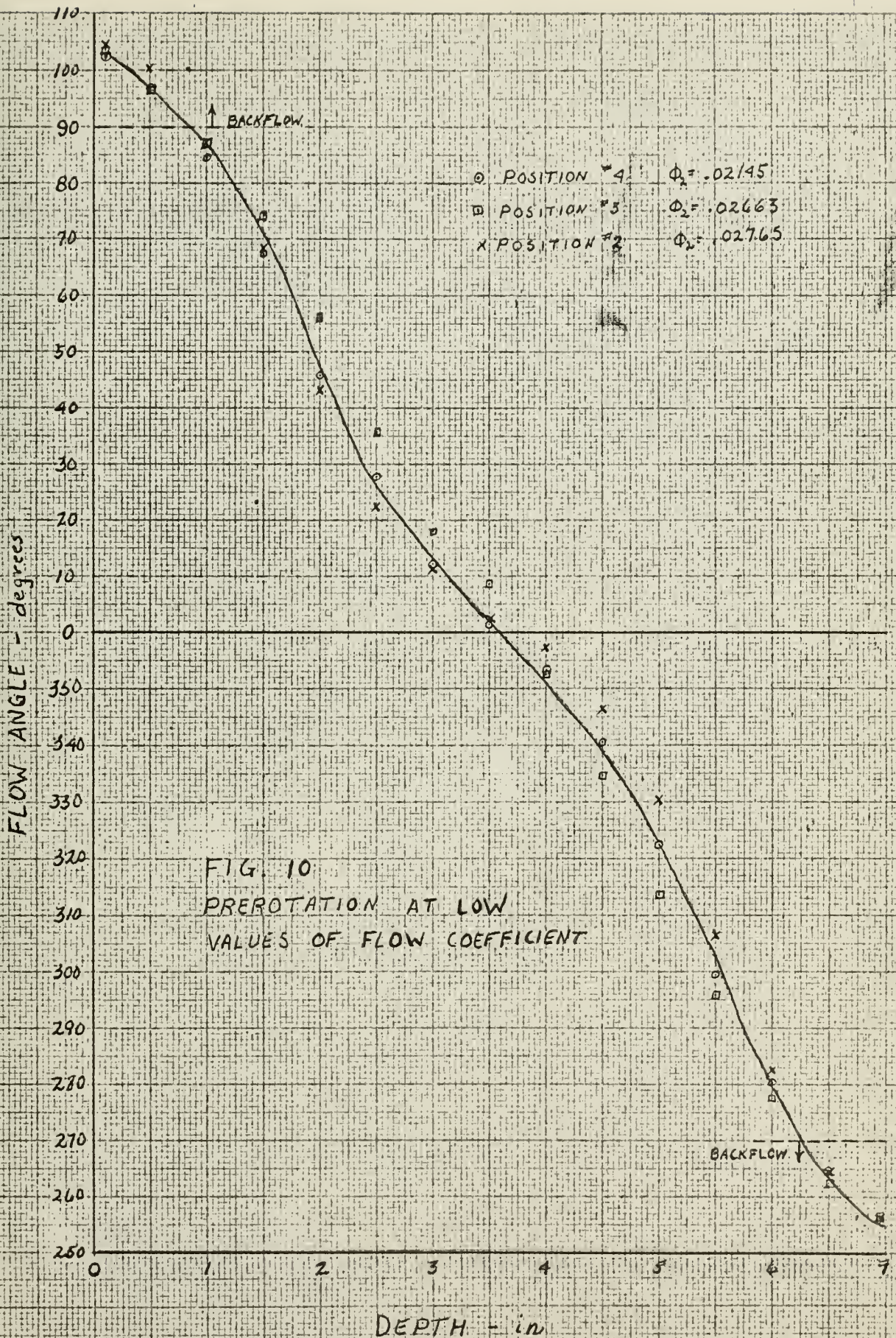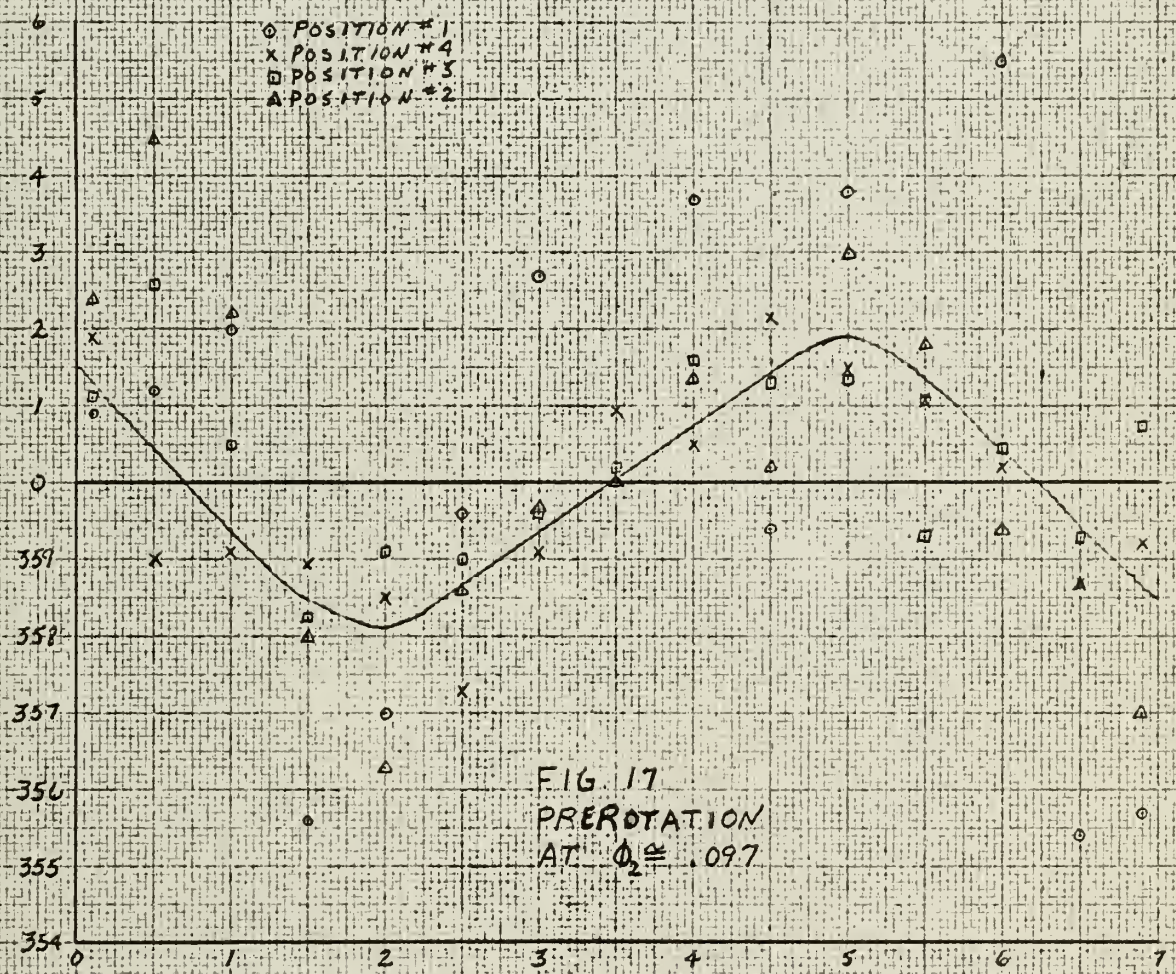
FIG. 11
PREROTATION AT POSITION
#1 AT $\phi_2 = .03853$

FLOW ANGLE — degrees

DEPTH — in

FIG. 12
PREROTATION
AT $\phi_2 \cong .048$

Legend:
⊙ POSITION #4
✕ POSITION #2

Axis labels:
FLOW ANGLE - degrees (vertical)
DEPTH - in (horizontal)

49

FIG. 13
PREROTATION
AT $\phi_2 = .065$

◎ POSITION # 4
✕ POSITION # 3
▢ POSITION # 2

DEPTH - in

FLOW ANGLE - degrees

FIG. 14
PREROTATION AT POSITION # 4
◎ $\phi_2 = .06336$
✕ $\phi_2 = .06138$

FIG. 15
PREROTATION
AT $\phi_2 \cong .078$

FIG. 16
PREROTATION
AT $\phi_2 \cong .087$

FIG. 17
PREROTATION
AT $\Phi_2 \cong .097$

POSITION #1
POSITION #4
POSITION #3
POSITION #2

FIG. 18
FLOW METER CALIBRATION CURVE

$Y = .543 + 9.35 \times 10^{-3} Rex - 1.65 \times 10^{-4} Rex^2 + 10^{-6} Rex^3$
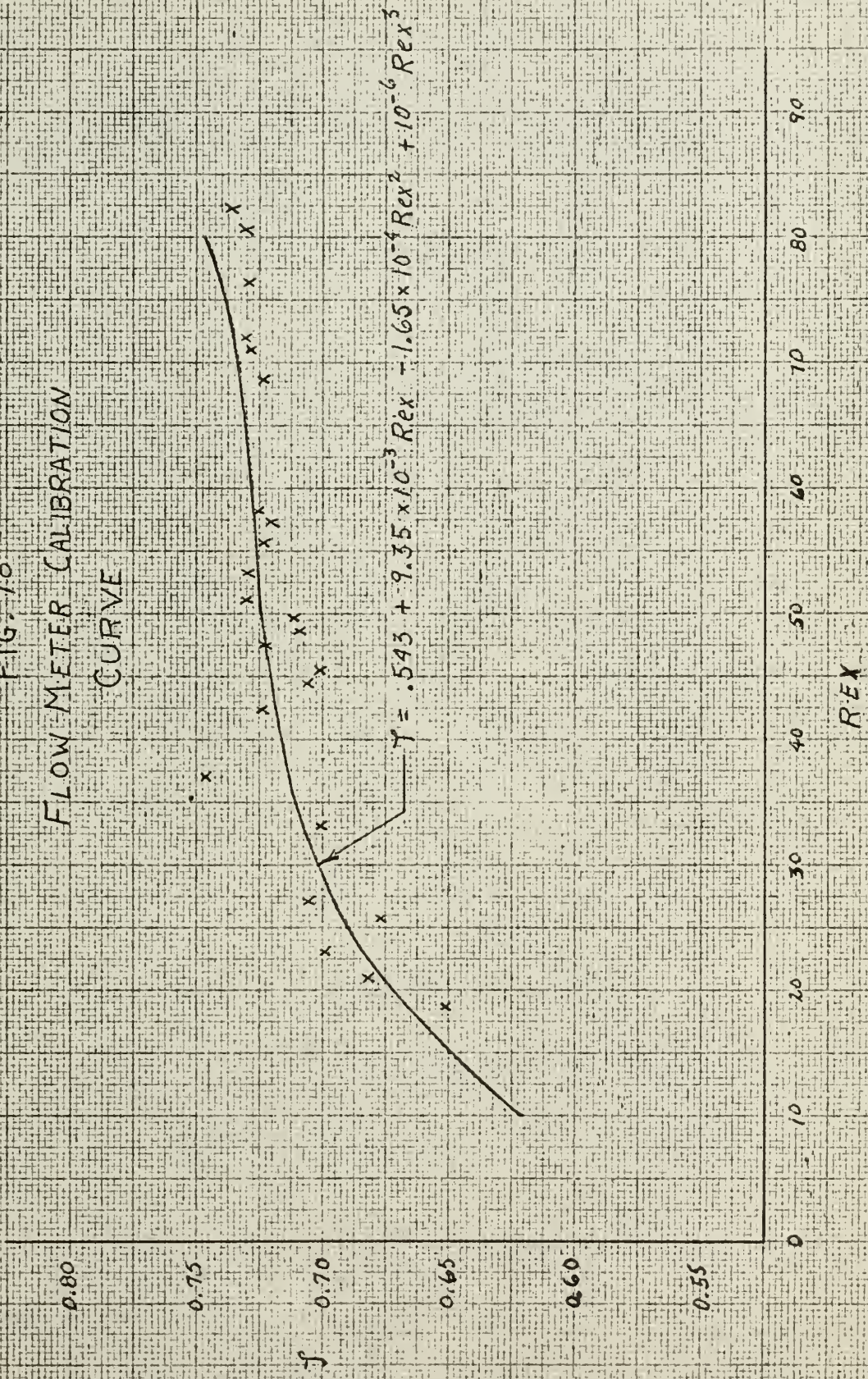
REX

53

FIG. 19.
Inlet Velocity Triangles
At Various Radii With
Prerotation Considered
At $\phi_2 \cong .026$

$W_1 = 79.5$
$V_1 = 33.6$
$29°$
$21.7°$
$U_1 = 90$
$\gamma = 1.17$

$V_1 = 33.6$
$W_1 = 114.4$
$57°$
$9.2°$
$U_1 = 141$
$\gamma = 1.83$

$85°$
$V_1 = 33.6$
$W_1 = 167$
$1°$
$U_1 = 200$
$\gamma = 2.6$

$103°$
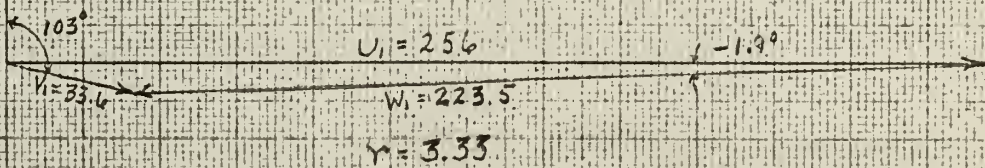$U_1 = 256$
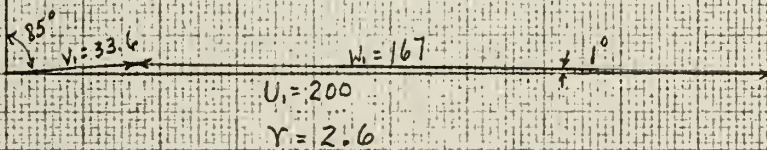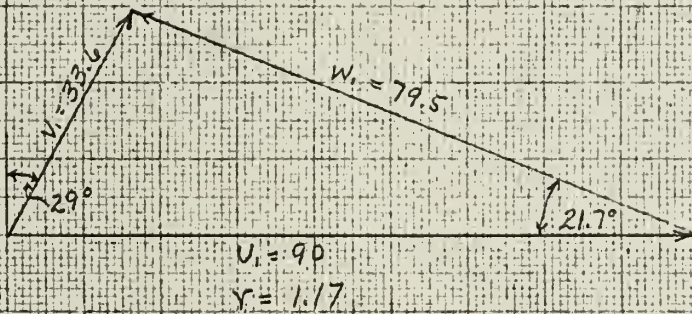$-1.9°$
$V_1 = 33.6$
$W_1 = 223.5$
$\gamma = 3.33$
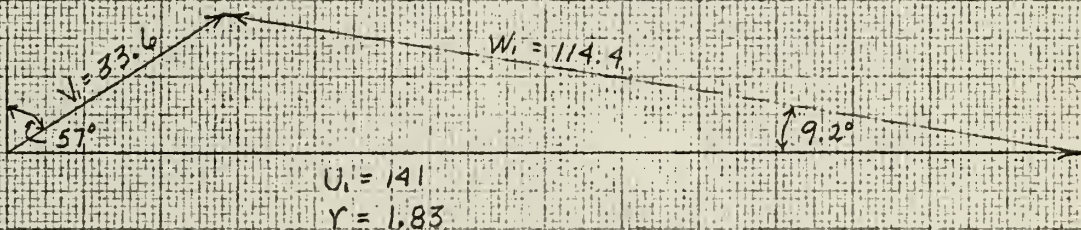
FIG. 20.
Inlet Velocity Triangles
At Various Radii With
Uniform Axial Flow
At $\phi_2 \cong .026$

$W_1 = 90.2$
$4.5°$
$V_1 = 7.1$
$U_1 = 90$
$\gamma = 1.17$

$W_1 = 141$
$2.9°$
$V_1 = 7.1$
$U_1 = 141$
$\gamma = 1.83$

$W_1 = 200$
$2°$
$V_1 = 7.1$
$U_1 = 200$
$\gamma = 2.6$

$W_1 = 256$
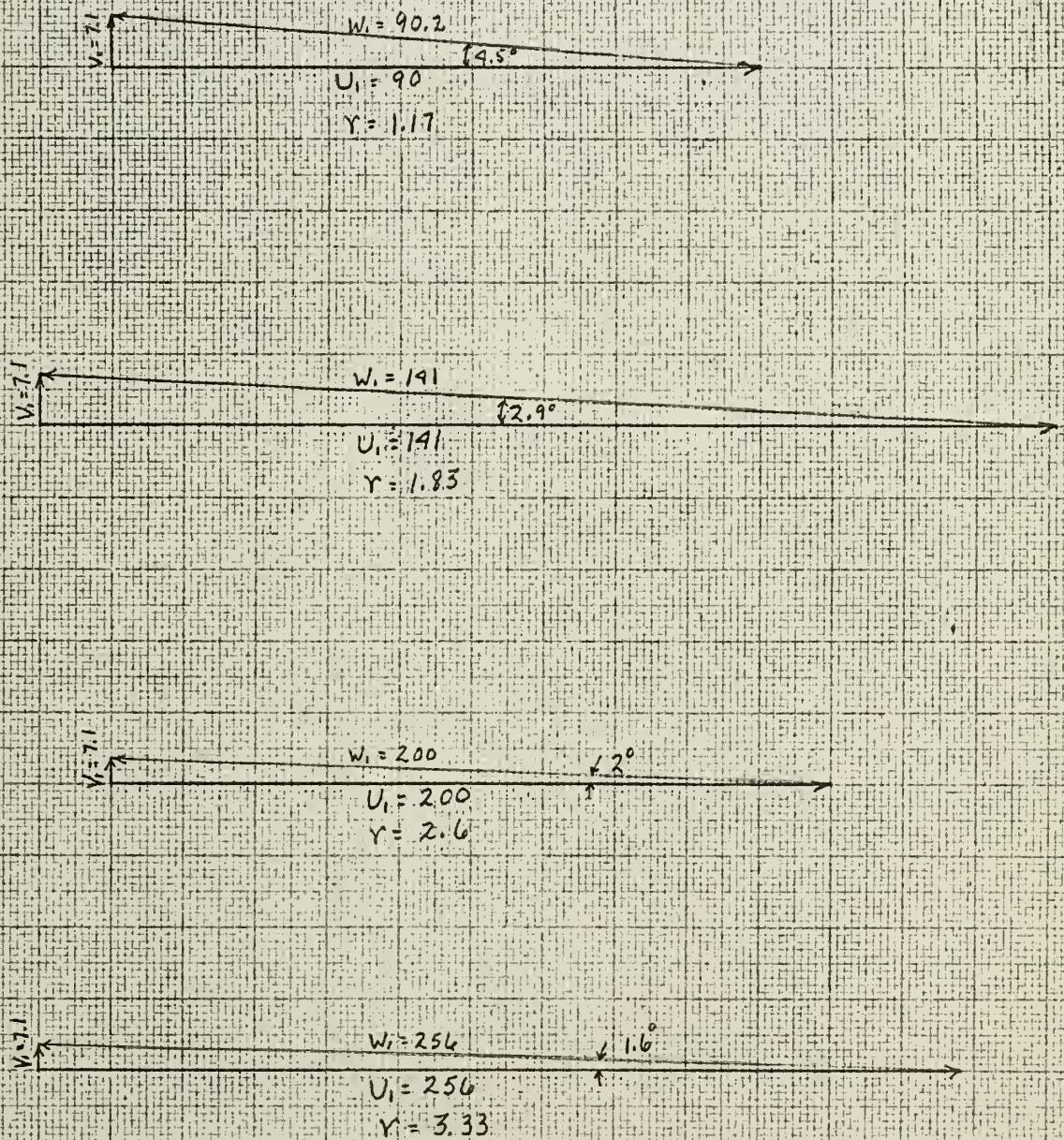$1.6°$
$V_1 = 7.1$
$U_1 = 256$
$\gamma = 3.33$

FIG. 21.
Inlet Velocity Triangles
At Various Radii With
Prerotation Considered
At $\phi_2 = .097$
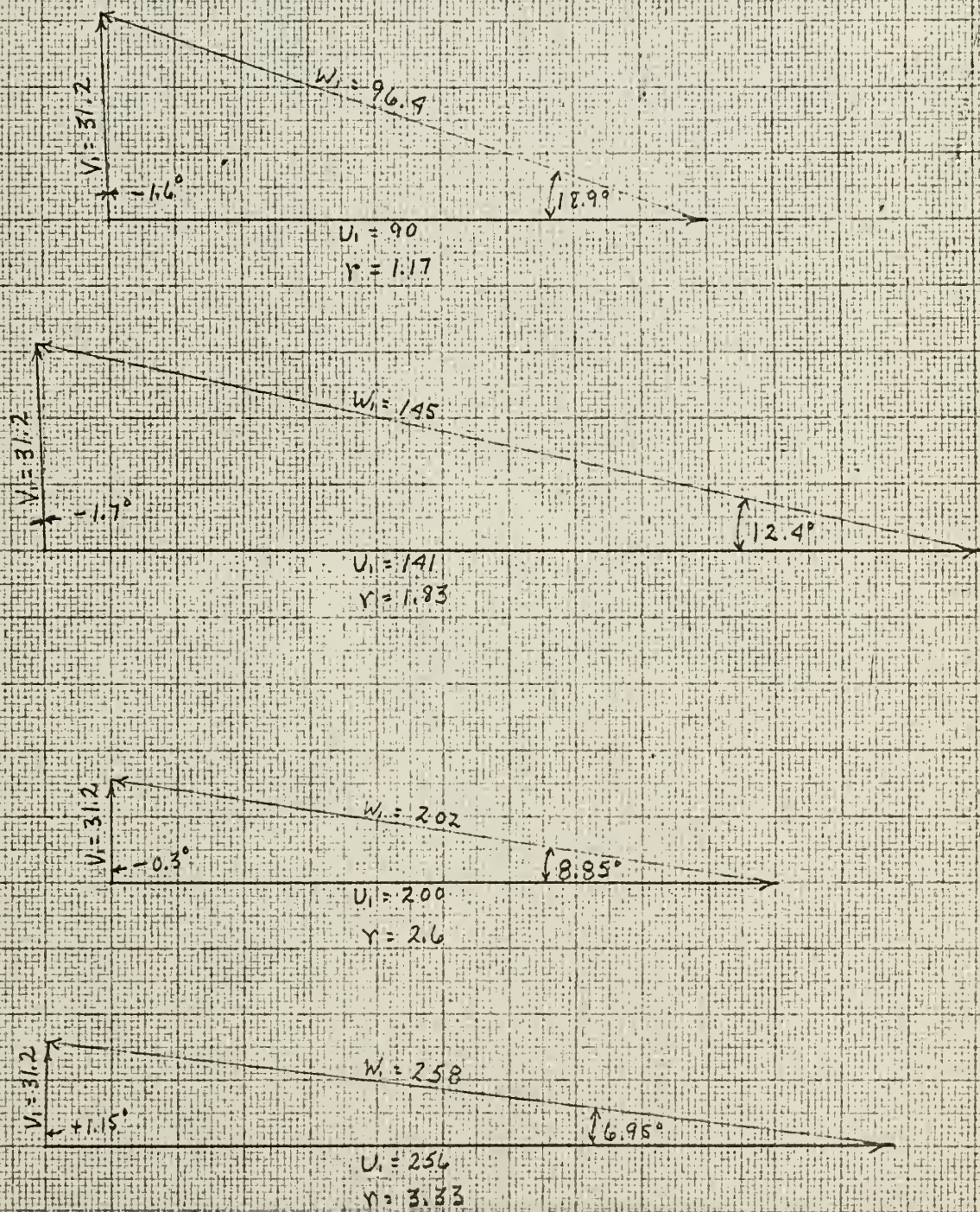
FIG. 22.
Inlet Velocity Triangles
At Various Radii With
Uniform Axial Flow
At $\phi_2 = .097$

$V_1 = 26.4$ $W_1 = 94.2$ $16.3°$
$U_1 = 90$
$\Upsilon = 1.17$

$V_1 = 26.4$ $W_1 = 193.5$ $10.6°$
$U_1 = 141$
$\Upsilon = 1.83$

$V_1 = 26.4$ $W_1 = 202$ $7.5°$
$U_1 = 200$
$\Upsilon = 2.6$

$V_1 = 26.4$ $W_1 = 258$ $5.9°$
$U_1 = 256$
$\Upsilon = 3.33$

57
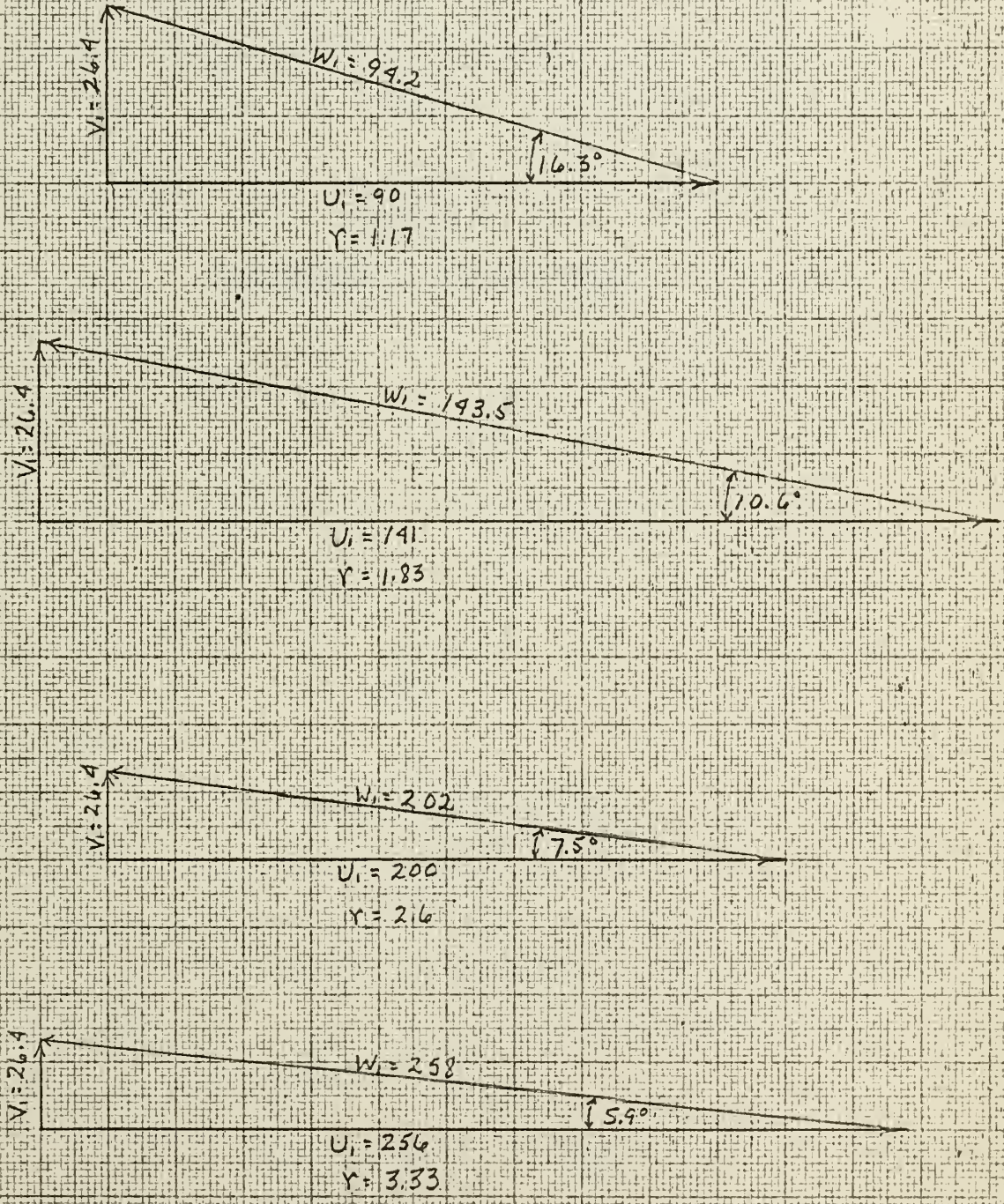
APPENDIX C

CALIBRATION OF THE FLOW METER

APPENDIX C

CALIBRATION OF THE FLOW METER

Since flow rates were very small without obstructions in the discharge line, it was felt that some method of determining flow rates with a minimum obstruction would best suit the purposes of this experiment. The only obstruction introduced into the flow in the flow meter devised was a Kiel probe. For purposes of calibration the discharge pipe was connected to an air supply line in which was installed a standard sharp-edged orifice type flow meter, so that all the air which passed through the standard meter also passed through the discharge pipe. The static pressure, P_s', the difference between the centerline total pressure and the static pressure, $\Delta P'$, and the centerline total temperature, T_2, were measured in the discharge pipe. Fig. 5. The following two equations were to be used for determining flow rate.

(1) $$\frac{P_s' V^2}{2gRT_2} = f \Delta P'$$

(2) $$w = \frac{P_s'}{RT_2} AV$$

combining,

(3) $$w = A(2\Delta P' f g P_s'/RT_2)^{\frac{1}{2}}$$

Everything can be measured except the factor f. The object of the calibration then is to determine f. This factor was not a constant so following the usual practice in flow meters, f was plotted as a function of Reynolds number. Fig. 18. In this graph a modified Reynolds number, Rex, was used, where,

$$Rex = Re/3600 = \frac{VD\rho}{3600\mu}$$

59

APPENDIX D

APPLICATIONS OF THE HOT WIRE ANEMOMETER

APPENDIX D

APPLICATIONS OF THE HOT WIRE ANEMOMETER

The hot wire anemometer operates on the principle that the resistance of most metal wire is a linear function of the temperature:

$$R = R_0 [1 + \alpha_0 (T - T_0)]$$

where, R_0 is the resistance at some reference temperature, T_0; and α_0 is the temperature coefficient of resistivity at that temperature.

It has also been found that, if a very fine wire is heated by an electric current and placed in a moving gas stream, the square of the current required to maintain a constant resistance in the wire is a linear function of square root of the product of the static pressure and the effective cooling velocity of the gas for Mach Nos. less than 0.3.

$$I^2 \propto (pV_e)^{\frac{1}{2}}$$

If β is the angle between the wire axis and the flow direction of the cooling gas, then:

$$V_e \cong V \sin\beta \qquad\qquad 45° < \beta < 135°$$

$$\text{or} \qquad V_e = V \sin\beta \ (1 - 1.2(D/L)^{\frac{1}{2}} \cos^2\beta) \qquad 5° < \beta < 175°$$

$$.0002 < D/L < .001$$

where, D/L is the ratio of diameter to length of the wire and V is the magnitude of the velocity of the cooling gas.

Thus if an air stream of known velocity and direction is available, a calibration curve may easily be obtained by taking a current reading with the hot wire in still air and another with the wire in the air stream. The two points may then be plotted, connected with a straight line and used as a calibration curve. Fig. 23.
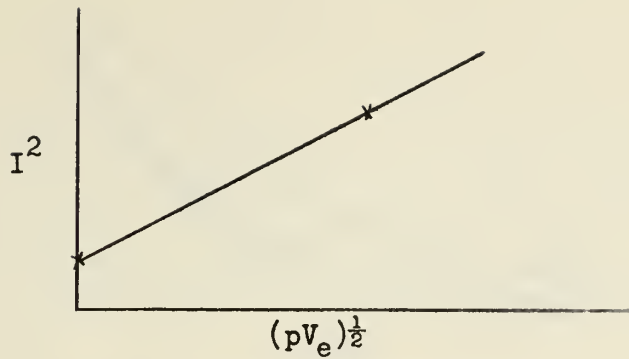
Fig. 23. Sample Calibration Curve

A Wheatstone bridge is normally used to observe the resistance in the hot wire and maintain it at a constant value. Fig. 24.
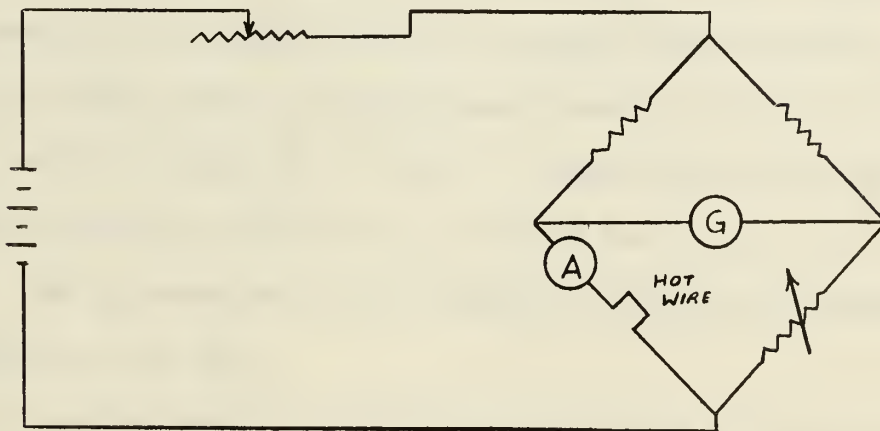

Fig. 24. Anemometer Circuit

Once a calibration curve is available the hot wire may be used to determine velocities of airstreams. It will be noted that for measuring velocity with the hot wire, a β of 90° should be used. V_e is then taken as the velocity because in this orientation the measured velocity is very insensitive to directional orientation of the wire.

If the current is held constant and the hot wire immersed in the moving gas stream, the resistance will vary as a function of the product of the static pressure and the effective cooling velocity of the gas. Fig. 25.
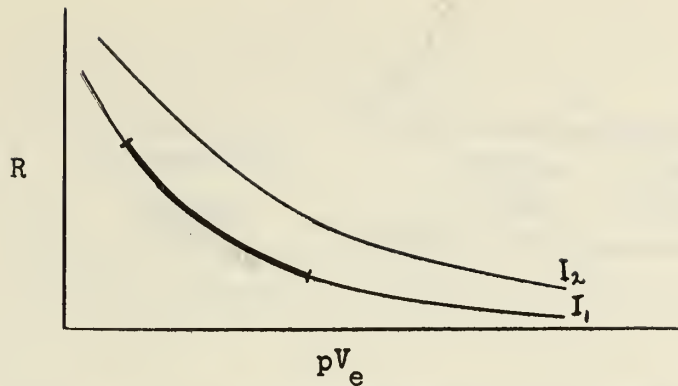
Fig. 25. Sample Characteristics Curve

This fact is useful in determining flow direction. For example, at a current of I_1, as β is varied through 360°, the resistance varies as indicated by the heavy lined portion of the above curve while the wire is immersed in a constant velocity, constant static pressure stream of gas. The minimum value of R would occur when $\beta = 90^\circ$, 270° and the maximum R would occur when $\beta = 0^\circ$, 180°. Another useful observation is that the resistance would be the same value for $\beta = 10^\circ$ as for $\beta = 350^\circ$. The galvanometer in the Wheatstone bridge will indicate the resistance of the wire.

It will be noted that the directional sensitivity of the hot wire is greatest for   near zero for two reasons:

(1) $\left| \dfrac{dR}{dV_e} \right|$ is greater for lower V_e

(2) $\dfrac{dV_e}{d\beta}$ is maximum near $\beta = 0$

To measure the flow direction no calibration is required except to determine the directional orientation of the hot wire axis with respect to some device for measuring angular displacement of the axis such as a protractor.

The hot wire elements are normally mounted on probes across two metal posts which are of a material which is readily soldered. Fig. 26.

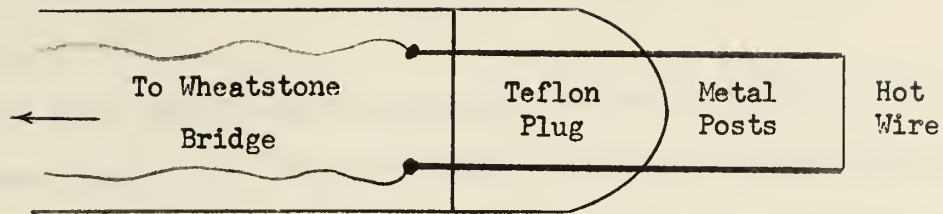To Wheatstone Bridge | Teflon Plug | Metal Posts | Hot Wire

Fig. 26. Hot Wire Probe

This arrangement fixes the wire axis approximately perpendicular to the probe axis. A protractor may be fixed to the probe in such a manner that, as the probe is rotated about its axis, the angular displacement from some reference position may be measured. By suitable calibration, any given orientation of the wire axis may be made to correspond to a known reading on the protractor.

Using this instrument the flow direction may be determined in the plane in which the wire is turned. To accomplish this, the probe is inserted into an airstream so that the probe axis is approximately perpendicular to the flow direction and rotated about its own axis. The resistance of the hot wire will vary, the maximum value being when the wire axis is in alignment with the component of velocity in the plane of the investigation. As an example, suppose the maximum resistance is observed when the protractor reads approximately 345°. It is difficult to tell exactly when the maximum resistance is encountered because the galvanometer needle is fluctuating. However, when the protractor reads 360°, the galvanometer needle fluctuates about a mark which will indicate some slightly smaller resistance. The needle fluctuates about this same mark when the protractor reads 331.2°. The protractor

reading for a maximum resistance should then be halfway between the two readings, or 345.6°.

It may be noted that it is not necessary for the two support posts to be the same length, Fig. 26, nor that the wire axis be perpendicular to the probe axis. The directional sensitivity suffers when the wire axis is not perpendicular to the probe axis, however.

One possible way of eliminating the effect of perturbation velocities would be to use a probe with two hot wires mounted in a cross fashion. Fig. 27. The two wires could be placed in different legs of the bridge so that effects of perturbations would be cancelling. After calibration in a known direction stream it could be used for direction determination. This instrument would also have double the sensitivity of a single wire.
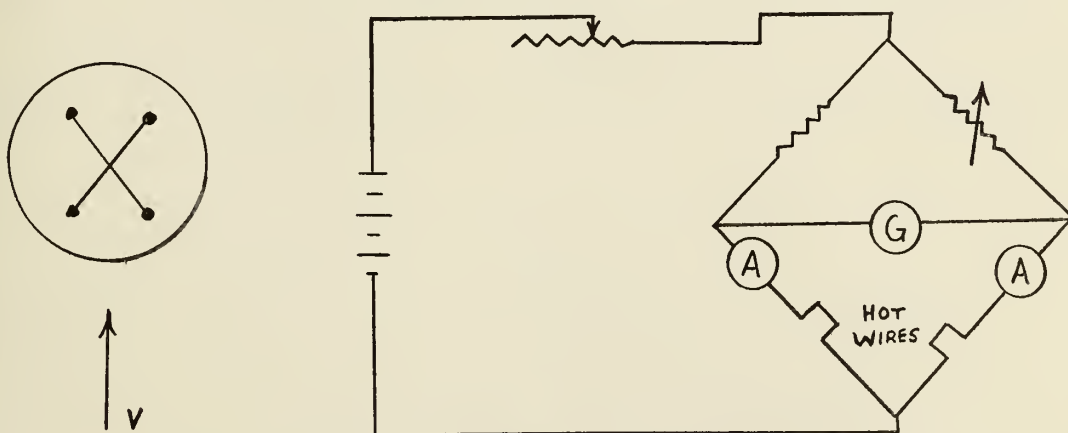

Fig. 27. Scheme For Using A Two Wire
Probe For Measuring Flow Direction.

APPENDIX E

THE COMPUTER PROGRAM

THE COMPUTER PROGRAM

A computer program was used to reduce the data and is included herein.

The following symbols were used in the program:

<u>Inputs</u>

N	run number
M	date
L	month indicator: +1 March, -1 April
NN	position no. where data was taken
P2	height of water column in tube to which pressure tap at outlet flange is attached - cm. of H_2O
PST	height of water column in tube to which static pressure line of flow meter is attached - cm. of H_2O
PATM	height of water column in tube open to atmosphere cm. of H_2O
DLP	difference between total and static pressure in flow meter - in. H_2O
T2	total temperature in air at flow meter - ^{o}C
BP	barometer reading - in. Hg
ALFA1	one of the angles read at each depth - degrees
ALFA2	the other angle read at each depth - degrees
TARE	the negative of flow angle read on the protractor at position #2 on the centerline of the inlet duct

<u>Outputs</u>

PHI2	flow coefficient
PSI2	pressure coefficient
Y	depth
ANGLE	flow direction

WI   mass flow rate at beginning of run

WE   mass flow rate at end of run

PSI2I   pressure coefficient at beginning of run

PSI2E   pressure coefficient at end of run

PHI2I   flow coefficient at beginning of run

PHI2E   flow coefficient at end of run

PRI   pressure ratio at beginning of run

PRE   pressure ratio at end of run

W   mass flow rate

PR   pressure ratio

ALFA   intermediate step in averaging process

Other in
Subroutine

P2A   pressure at discharge flange of pump - PSF

A2   discharge area of impeller - ft^2

U2   impeller peripheral speed - ft/sec

R   gas constant

PSTA   flow meter static pressure - PSF

TT2   same temperature as T2 - $^{\circ}$R

BPA   barometric pressure - PSF

RHO   density at flow meter - lbm/ft^3

ZETA   flow rate factor

T2F   same temperature as T2 - $^{\circ}$F

Z   viscosity of air in flow meter

VAV   average velocity in flow meter - ft/sec

A   cross-sectional area of discharge pipe - ft^2

REX   modified Reynolds number in discharge pipe

WREF   referred flow rate - ft^2

68

For each run, this program requires seven data cards. On the first card, the values of N, M, L and NN are entered in four fixed point fields of ten. The second and third cards are six floating point fields of ten in which are entered the values obtained for P2, PST, DLP, T2, PATM, and BP. The second card contains those values measured at the beginning of the run and the third card, those values measured at the end of the run. The next four cards contain eight floating point fields of ten. The first of these contains the values of ALFA1(1) through ALFA1(8). The second contains the values of ALFA1(9) through ALFA1(15) and TARE. The last two cards are the same as cards four and five, except substitute ALFA2 for ALFA1.

The program first enters the subroutine twice to compute flow coefficient and pressure coefficient from the data on cards two and three. It first changes all pressures to PSFA and temperature to °R. If different manometers and thermometers are used, some of the constants may require change. It then does two iterations to find W because of the interdependence of W and ZETA. The formula for ZETA in terms of REX should not be used for REX greater than 70. Fig. 17. The subroutine then computes the pressure coefficient and the flow coefficient.

The flow coefficients and pressure coefficients at the beginning and end of the run are then averaged. The first part of the table is then printed. Next the two angles measured for each depth are averaged and printed with its corresponding depth.

```
      PROGRAM PREROT
      DIMENSION Y(15),ALFA1(15),ALFA2(15),ANGLE(15)
      Y(1)= 0.1
      DO 20 J=2,14
      A=J-1
 20   Y(J) = 0.5 * A
      Y(15) = 6.9
 25   READ 99, N,M,L,NN
      CALL FLOW (WI,PSI2I,PHI2I,PRI)
      IF(PRI)7,7,6
  6   CALL FLOW (WE,PSI2E,PHI2E,PRE)
      W=(WE+WI)/2.0
      PR=(PRE+PRI)/2.0
      PSI2=(PSI2I+PSI2E)/2.0
      PHI2=(PHI2I+PHI2E)/2.0
      PRINT 110
      PRINT 111,N
      PRINT 112
      IF(L)21,21,22
 21   PRINT 121,N,M
      GO TO 23
 22   PRINT 122,N,M
 23   PRINT 123,NN
      PRINT 124, PHI2,PSI2
      PRINT 125
      READ 300, ALFA1, TARE
      READ 300, ALFA2, TARE
      DO 30 K=1,15
      ALFA= ALFA1(K)+ALFA2(K)    + 2.0*TARE
      IF(ALFA-360.0)1,2,3
  1   IF(ALFA-270.0)4,4,2
  2   ALFA=ALFA + 360.0
      GO TO 4
  3   IF(ALFA-450.0)5,5,4
  5   ALFA = ALFA - 360.0
  4   ANGLE(K)=ALFA/2.0
 30   PRINT 200, Y(K), ANGLE(K)
      GO TO 25
110   FORMAT(1H1/////////)
111   FORMAT(38X6H TABLE I3///)
112   FORMAT(34X20H PREROTATION TEST          ///)
121   FORMAT(14X8H RUN NO. I3,31X I5,11H APRIL 1964 ///)
122   FORMAT(14X8H RUN NO. I3,31X I5,11H MARCH 1964 ///)
123   FORMAT(35X13H POSITION NO. I2///)
1240  FORMAT(14X19H FLOW COEFFICIENT =  F7.5,
     13X23H PRESSURE COEFFICIENT = F7.5///  )
125   FORMAT(32X6H DEPTH 9X6H ANGLE ///)
200   FORMAT(32XF6.2,9XF6.2//)
99    FORMAT(4I10)
300   FORMAT(8F10.0)
  7   STOP
      END
      SUBROUTINE FLOW (W,PSI2,PHI2,PR)
      READ 100 , P2, PST, DLP, T2, PATM, BP
      IF (BP)9,9,8
  8   P2A=((PATM-P2)/ 34.544+BP)*70.727
      A2= .1453
      U2= 424.19
      R=53.35
      PSTA=((PATM-PST)/34.544 +BP)*70.727
      DLPA= DLP *5.2
      TT2 = (T2 + 40.)*1.8 +420.
      BPA = BP*70.727
      RHO = PSTA/(R* TT2)
      PR  = P2A/BPA
      ZETA = .7
      VAV = SQRTF(64.348 * ZETA * DLPA/RHO )
      A =   3.14159/ 64.0
      W =   RHO * A * VAV
      T2F= TT2- 460.0
      Z=.0162 + .000029 *T2F -.00000001 *T2F*T2F
      REX = 2.1053 * W/ Z
      ZETA = .543 + .00935*REX -.000165*REX*REX +.000001*REX**3
      VAV = SQRTF(64.348*ZETA * DLPA/RHO)
      W=   RHO * A * VAV
      WREF = SQRTF(R* TT2/32.174) * W /BPA
      PSI2=(P2A-BPA)*32.174*R*TT2/(U2*U2*P2A)
      PHI2= W*R*TT2/(U2*P2A*A2)
      GO TO 11
  9   PR = 0.0
 11   RETURN
100   FORMAT ( 6F10.0)
      END
      END
```

70

Thesis 72731
Ô83 Osgood
    An investigation of
the prerotation
characteristics of a
fluid...